Rethinking termite methane emissions: does the mound environment matter?

Abbey R. Yatsko[1]*, Paul Eggleton[2], Caleb Jones[3], Marcos Pérez-Losada[4], Ignacio Ramos-Tapia[5], Jeff R. Powell[6], Baptiste Wijas[7], Amy E. Zanne[7]

[1] Biology Department, University of Miami, University of Miami, Coral Gables, Florida, USA
[2] Life Sciences Department, The Natural History Museum, London, UK
[3]ArborMeta, Byron Bay, NSW, Australia
[4] Milken Institute School of Public Health, The George Washington University, Washington, D.C., USA
[5] Center for Bioinformatics and Integrative Biology, Facultad de Ciencias de la Vida, Universidad Andres Bello, Republica 330, Santiago, Chile
[6] Hawkesbury Institute for the Environment, Western Sydney University, Penrith, New South Wales, Australia
[7] Cary Institute of Ecosystem Studies, Millbrook, New York, USA

*Corresponding author: ayatsko1@gmail.com

Abstract

Termites are important decomposers in tropical ecosystems, and they emit methane (CH_4) from digesting plant matter. Termite contributions to global CH_4 emissions are calculated using species-specific termite CH_4 emissions from individuals (termite emission factors; TEF) and estimated biomass, which overlooks how the termite mound environment may alter emissions to the atmosphere. Factors such as feeding habits, mound methanotrophs, mound structural traits (size, wall thickness), and environmental conditions (temperature, season) can influence net CH_4 emission but remain unparameterized.

We investigated how these factors shaped CH_4 emissions from three dominant mound-building termite species (*Coptotermes acinaciformis*, *Nasutitermes magnus*, and *Amitermes laurensis*) in a northern Australian savanna across four seasons. We compared species-level TEFs and emissions at the mound and landscape scales to assess species relative contributions with and without accounting for mound environment. We expected larger and thinner-walled mounds would emit greater CH_4, while emissions would also be higher at high temperatures and during wet seasons. Finally, we expected greater emissions with a lower abundance of methanotrophs and *pmoA* (responsible for reducing CH_4) gene copies in the mound material.

Coptotermes acinaciformis individuals had the highest TEFs (1.07 μg CH_4 g^{-1} termite h^{-1}), while *N. magnus* mounds emitted the most CH_4 (3,426 μg CH_4 h^{-1} m^{-2}) and *A. laurensis* had the highest emissions at the landscape scale (1.04×10^{-9} Tg CH_4 ha^{-1} yr^{-1}). CH_4 emissions increased with temperature and were highest in the wet-to-dry transition season. Surprisingly, bacterial methanotroph communities and *pmoA* gene abundance had no direct effect on CH_4 emissions. Our results highlight the limitations of using TEFs to estimate the global contributions of termites to atmospheric CH_4 emissions and emphasize incorporating the mound environment when calculating net termite CH_4 emissions. This information allows more accurate parameterization of termite CH_4 contributions to savanna carbon cycling and global CH_4 budgets.

Keywords: termite, methane emissions, temperature, Australian savanna, termite emission factor, termite mound structure

Introduction

Termites are key decomposers, especially in the tropics, dominating terrestrial arthropod biomass at an estimated global biomass of 100 Mt (Rosenberg et al., 2023) and cycling significant quantities of terrestrial carbon (Seibold et al., 2021; Griffiths et al., 2019). As a by-product of carrying out decomposition, termites release carbon dioxide (CO_2), but also methane (CH_4). CH_4 is produced by symbiotic methanogens (Archaea) in termite guts as they break down wood, nutrients in soils, and dead plant matter (Zimmerman et al. 1982; Brune & Dietrich 2015). CH_4 is a powerful greenhouse gas that contributes to climate warming (IPCC 2021), but there exist many uncertainties in quantifying natural CH_4 sources (i.e., emissions) and sinks (i.e., removal, conversion, or storage) that comprise the CH_4 budget (Kirschke et al. 2013; Saunois et al. 2020). Termite CH_4 is one such poorly parameterized component of the global CH_4 budget; current estimates show that termites emit 8-21 Tg CH_4 per year (Ito 2023). However, this value is highly debated (Zimmerman et al., 1982; Saunois et al., 2020), since variation in termite ecology is not captured in present estimates (Law et al., 2024a). To resolve such uncertainties, a more nuanced understanding of the underlying factors contributing to termite CH_4 emissions is required (Law et al., 2024a).

Estimates for global termite CH_4 emissions are typically derived by multiplying a termite emission factor (TEF: average CH_4 emission per termite biomass, μg CH_4 g^{-1} termite h^{-1}) by regional-scale estimates of termite biomass (Ito 2023; Saunois et al., 2020). Species variation in TEFs spans a wide range, from negligible emissions to more than 25 μg CH_4 g^{-1} termite h^{-1}, which is largely attributed to differences in feeding groups (Sanderson 1996; Zhou et al., 2022) and termite gut microbial composition (i.e., the presence of CH_4-producing Archaea, Rouland et al., 1993). It has been shown that soil feeders (*Cubitermes*

sp.) and grass feeders (*Trinervitermes* sp.) have high TEFs (Sanderson 1996; Zhou et al., 2022), potentially due to higher archaeal-to-bacterial ratios in their guts (Rouland et al., 1993; Arora et al., 2022). Additionally, accurately estimating global termite biomass is a challenging venture, due to the diverse sizes and constructions of termite colonies, including epigeal (above ground) mounds, subterranean colonies, arboreal nests, and colonies in deadwood (Law et al., 2024a).

Termite contributions to global CH_4 emissions are therefore estimated using an overly simplistic model that fails to capture the complexities of how termite ecology influences net CH_4 emission to the atmosphere (Law et al., 2024a). This failure is especially true when considering mound-building termites, which are important decomposers of wood, soil, plant litter, and grass particularly in savanna ecosystems (Zanne et al., 2022; Bunney et al., 2024). Tropical savannas often feature large epigeal termite mounds (in Africa: Meyer et al., 1999; Davies et al., 2014, in Australia: D'hont et al., 2021, in South America: Neto et al., 1986, in India: Jouquet et al., 2015), sometimes covering up to 5-7% of the land area (Levick et al., 2010; Holdo & McDowell 2004). In this way, termite mounds represent a concentration of termite biomass and CH_4 emission (Jamali et al., 2011a; Brümmer et al., 2009; van Asperen et al., 2021; Räsänen et al., 2023), which can overcome the oxidative capacity of soils, which are recognized as CH_4 sinks (Eggleton et al., 1999; Dunfield 2007). However, current CH_4 calculations fail to integrate how the termite mound structure itself, local environmental conditions, and mound microbial communities shape CH_4 release.

Structural traits of termite mounds shape the capacity for internal gas exchange and diffusion to the atmosphere (Ocko et al., 2019). Wall thickness is one such trait that varies widely across species and environmental conditions (Korb 2011). Greater wall thickness, while more protective from the outside environment and organisms trying to access the mound, can limit diffusion and result in an accumulation of gases, such as CO_2, inside the mound (Korb 2003). Further, when termite mounds grow, they can support a larger termite population (Josens & Soki 2010), with potential to generate higher total mound CH_4 emissions (van Asperen et al., 2021; Jamali et al., 2011b; Vesala et al., 2023). Therefore, identifying how wall thickness and mound size influence CH_4 emission will provide insight on the importance of incorporating these factors in CH_4 upscaling efforts.

Additionally, environmental conditions such as temperature and season influence termite activity and CH_4 emissions. Termite wood decomposition rates are highly sensitive to increasing temperatures, which could result in increased CH_4 emissions (Zanne et al., 2022, Law et al., 2024b). Direct relationships between termite CH_4 emission, decomposition activity, and temperature remain unexamined, but previous research suggests that mound CH_4 emissions are highest at the warmest part of the day (Jamali et al., 2011a, Räsänen

et al., 2023). Seasonality has also been shown to affect termite mound CH_4 emissions: previous research in an Australian tropical savanna showed significantly higher mound CH_4 emission during the wet season than for other times of the year (Jamali et al., 2011a), which could be due to changes in termite biomass (Jamali et al., 2011b) or temperature. However, other studies found mound emissions to be highest in the dry season (Quevedo et al., 2021; Räsänen et al., 2023), which could result from decreased oxidation of methane by microbial activity resulting from moisture limitations. Determining the role of temperature and seasonality in termite mound CH_4 emissions is therefore necessary for accurate annual CH_4 emission estimates.

Finally, CH_4 released from individual termites residing within a mound may not reach the atmosphere due to the presence of methanotrophic (CH_4-consuming) bacteria and archaea within termite mounds. Methanotrophic bacteria have been shown to reduce the net emission of CH_4 from the mound to the atmosphere by 50% (Nauer et al., 2018a). The mound microbial community can therefore influence net CH_4 emission, which is known to vary across termite species (Ho et al., 2013; Chiri et al., 2020). The gene encoding the particulate methane monooxygenase subunit A (*pmoA*) is involved in the CH_4 oxidation pathway for most bacterial methanotrophs (Cupples & Thelusmond 2022). The *pmoA* gene plays an important role in CH_4 metabolism and its abundance in termite mound material is a standard method for identifying methanotrophic microbe communities (Chiri et al., 2020). However, direct associations between methanotroph community composition, *pmoA* gene abundance, and termite mound CH_4 emission are yet to be tested.

In this study, our goal was to refine our understanding of termite contributions to CH_4 emissions by parsing out various factors that influence net mound CH_4 emission to the atmosphere. To do so, we combined previous measures of mound abundances (Clement et a1., 2021) with new measures of species-level TEFs and mound-level CH_4 emissions from three prominent mound-building termite species, with varied feeding habits and mound traits, in North Queensland, Australia tropical savannas. We asked the following questions: 1. How do species-level TEFs contrast with average mound-level CH_4 emissions and landscape-scale CH_4 emissions? 2. What is the relative influence of species-specific mound structural traits (mound size and wall thickness) and environmental drivers (temperature and season) on mound-level CH_4 emissions? 3. Do methanotrophic microbial communities (archaea and bacteria) and methanotroph gene (*pmoA*) abundance in the mound material influence CH_4 emission within and across termite mounds?

Methods

Study site

Termite mounds were sampled at the Australian Wildlife Conservancy (AWC) Brooklyn Sanctuary in the Station Creek region (-16.61 S, 145.24 E, Figure 1). The Station Creek region comprises a wet savanna ecosystem with distinct wet and dry seasons, experiencing 1,728 mm of rainfall annually (Cheesman et al., 2018). Floristically, the region is dominated by *Eucalyptus cullenii*, *Corymbia clarksoniana, Acacia disparrima* subsp. *Calidestris* and *Larsenaikia ochreata* (Flores-Moreno et al., 2024). Termite diversity and abundance in this region is relatively high for savanna ecosystems, with 14 species described to occur in the area (Clement et al., 2021). *Amitermes laurensis*, *Coptotermes acinaciformis*, and *Nasutitermes magnus* are abundant mound-building termite species (Clement et al., 2021) and were selected as the focal species of this study. *Coptotermes acinaciformis* feeds on wood, and typically builds medium to large-sized mounds with a dome shape (mean height = 87 cm, Clement et al., unpublished data), which are often built at the base of trees which they frequently hollow (Yatsko et al., 2024; Yatsko et al., 2025). *Nasutitermes magnus* feeds on grass and builds large mounds (mean height = 92 cm, Clement et al., unpublished data). *Amitermes laurensis* feeds on plant litter and builds small conical mounds (mean height = 59 cm, Clement et al., unpublished data) that have high abundance in the landscape (see Figure 1 for mound morphologies).

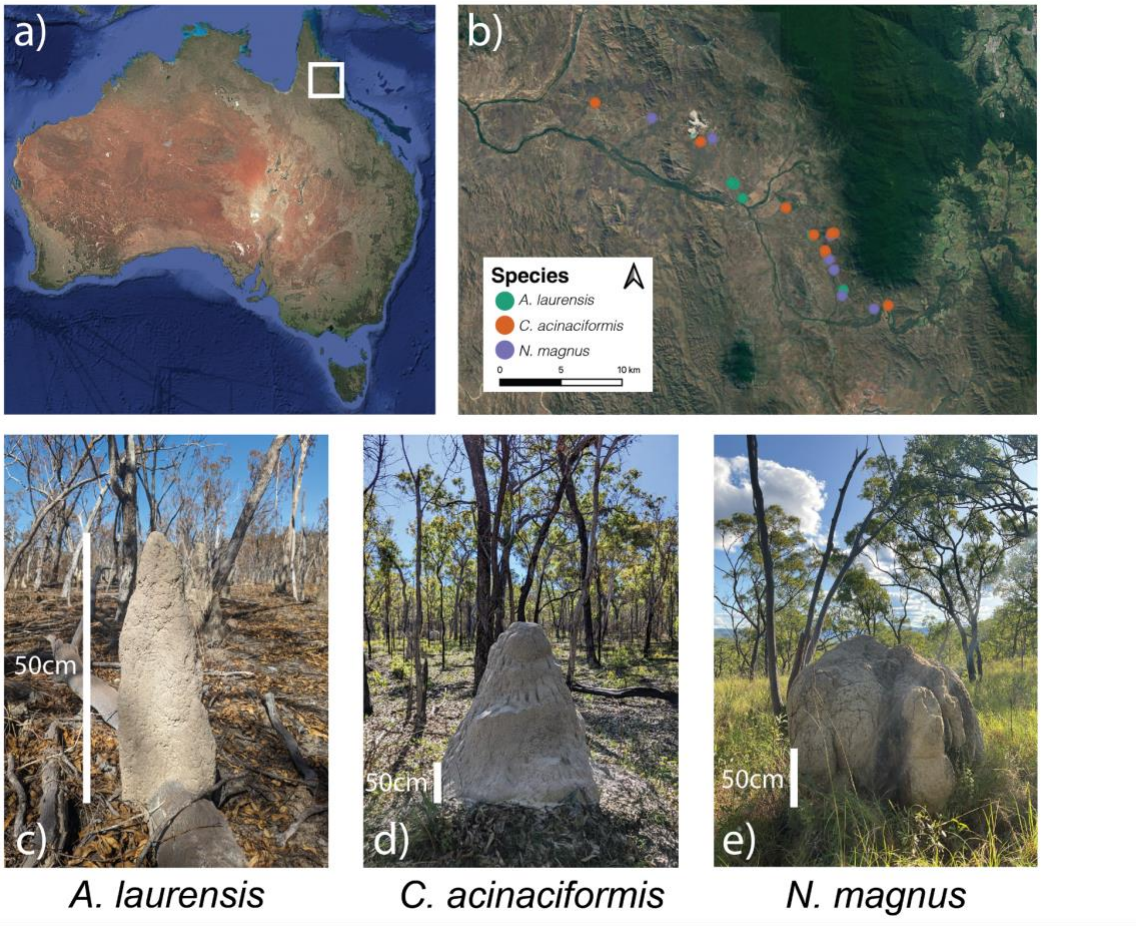

Figure 1. a) Study location in far North Queensland, Australia (white square). b) Location of sampled termite mounds repeatedly measured across all four seasons (n = 19, colored by species) in the greater Station Creek region. Termite mound morphologies common to c) *A. laurensis*, d) *C. acinaciformis*, e) *N. magnus*. White scale bars on each species mound morphology image indicate a reference height measurement of 50 cm.

Determining species-level termite emission factor

In February 2024 we collected mound material from the field and conducted laboratory measurements to calculate a TEF for each species. To do so we removed entire *A. laurensis* mounds (n = 5) from the field due to their small size. For *C. acinaciformis* (n = 5) and *N. magnus* (n = 5), mounds were too large, so we subsampled mound pieces using a saw and chisel. Mound samples were placed in a bucket and transported back to laboratory conditions where they equilibrated to room temperature (24°C) for a minimum of 12 hours prior to CH_4 emission measurement. We cut mound samples into smaller pieces (approximately 5x5 cm) and removed all termites from the mound piece (mean termite biomass = 2.2 g) to measure CH_4 emissions directly from termite individuals. We measured CH_4 emissions using a Los Gatos Research (LGR) Ultraportable Greenhouse Gas Analyzer (UGGA, San Jose, CA, United States) connected to a closed sampling chamber (LI-COR 8200-104, Lincoln, Nebraska, United States). Termite biomass (g) was used to calculate the species-level TEF, defined as mean μg CH_4 g termite^{-1} h^{-1} (Zhou et al., 2022).

Termite mound CH_4 emission sampling

Termite mound CH_4 emissions were sampled four times between May 2022 and February 2024 to capture the range of seasonal conditions and temperatures characterizing the savanna ecosystem (Supplementary Table 1). We selected mounds for each of the three termite species based on the following criteria: a) mounds were accessible by vehicle across weather conditions, b) mounds were active and occupied by termites at the time of measurement, c) mounds were representative of the range of sizes for a given species, and d) mounds were in locations with low likelihood of human interference. The location of each mound was recorded with GPS coordinates (Figure 1).

The initial survey in May 2022 (wet-to-dry transition season) targeted a larger number of mounds per species (*A. laurensis*: n= 14, *C. acinaciformis*: n = 25, *N. magnus*: n = 21, Supplementary Table 2). Then, eight mounds from each species were randomly selected from the May 2022 campaign for remeasurement in November 2022 (dry-to-wet season transition), August 2023 (mid-dry season), and February 2024 (mid-wet season). Over the course of sampling, there were five instances where mounds died or were destroyed and could not be re-measured (Supplementary Table 2). When this was the case, the mound was replaced

with a mound closest in size from the original May 2022 sampling pool. In February 2024, we were only able to re-measure seven *N. magnus* mounds due to logistical constraints of accessing mounds following Cyclone Jasper which affected the region in December 2023. At the end of the experiment, seven *A. laurensis*, seven *C. acinaciformis,* and five *N. magnus* mounds were re-measured during all four seasons (Supplementary Table 2). These mounds were used to analyze the effect of season and temperature on mound CH_4 emission.

Termite sampling and identification

Two soldiers and five workers were sampled from each mound in the May 2022 campaign and stored in 95% ethanol. Soldier sample morphology was used to confirm species-level identification (P. Eggleton, personal communication, May 2023). When visual identification was not possible, we followed the protocol in Clement et al. (2021) for species identification using DNA barcoding.

Field-based measurements of termite mound CH_4 emissions

We sampled CH_4 emissions from termite mounds in the field using a semi-closed chamber-based sampling system connected to the LGR UGGA (Supplementary Figure 1). For each mound, 4-5 surface measurements were taken by attaching the LGR UGGA to a semi-closed PVC sampling chamber (Jeffrey et al., 2020) via gas tubing. Sampling chambers were placed on the mound surface without breaking the mound wall (Supplementary Figure 1a) and secured with an external airtight seal using a ring of inert potting clay (Walker Ceramics, Bayswater, VIC, Australia; Jeffrey et al., 2020, Supplementary Figure 1b).

Sampling chambers were fixed on the flattest surface of the mound to accurately calculate chamber volume which was approximated as a cylinder. Different sized chambers were used for the three species, as *A. laurensis* mounds were smaller (chamber volume = 2,960.1 cm^3, surface area = 183.9 cm^2) and *C. acinaciformis* and *N. magnus* mounds could fit medium chambers (chamber volume = 899.9 cm^3, surface area = 83.3 cm^2). We standardized the mound sampling points to optimize for the unique geometries of each mound. *Coptotermes acinaciformis* and *N. magnus* mounds were sampled in five locations: north-facing side at 50% mound height, east-facing side on the flattest surface closest to the mound base, south-facing side at 50% mound height, west-facing side on the flattest surface closest to the base, and the top of the mound at the flattest surface (Supplementary Figure 1c). Due to their conical shape, *A. laurensis* mounds were sampled in the first four locations but with the top measurement omitted, since there was no flat surface available. Individual sampling points were marked so that the sampling position could be repeated during remeasurement.

After chambers were fixed to the mound and sealed with clay, CH_4 emission was recorded for 120 s and internal chamber air temperature (°C, temperature at the mound surface) was simultaneously recorded every minute using a thermocouple probe (PerfectPrime TC41, 4-Channel K-Type Digital Thermometer Thermocouple Sensor). All measurements were made between 08:00 and 17:00. Measurement quality assessed using two criteria: 1) no humming noise coming from the sampling chamber, which indicated that the clay ring seal was airtight and free of leaks (Jeffrey et al., 2020), and 2) real-time measurements on the LGR UGGA displayed positive, linear slopes, indicating constant production of CH_4 and no leaks.

CH_4 emission calculation

CH_4 emissions from termite mounds and individual termites (μg CH_4 h^{-1}) were calculated using linear regression slopes (x = time, y = [CH_4] in chamber headspace) following the ideal gas law and using average chamber air temperature for each measurement and assuming ambient pressure. R^2 and p-values were calculated for each measurement, and samples with $R^2 < 0.4$ were manually inspected for erroneous points. Erroneous points often were present at the beginning or end of the measurement due to the chamber opening or closing, and were omitted when present.

Positive slopes indicated net CH_4 emission, while negative slopes indicated that CH_4 oxidation exceeded production. In our data collection and analysis, we only considered termite mounds to be alive if the average mound emission was a positive value. However, within an individual mound it was possible for some subsamples to show negative slopes, indicating net CH_4 oxidation. For analyses where subsampled emissions were the unit of measure (i.e., mound microbial communities, see below), we included negative emissions. For analyses run at the mound level (i.e., structural equation modeling, see analyses below), we only considered live mounds and therefore CH_4 emission was always positive. CH_4 emissions for each subsample were divided by the surface area covered by the sampling chamber to derive emissions per unit area (μg CH_4 h^{-1} m^{-2}). Total mound emission was derived by multiplying average mound emission per unit area by total surface area of the mound (μg CH_4 h^{-1} $mound^{-1}$).

Mound size measurement

We used photogrammetry to estimate mound surface area and volume. Photogrammetry uses multiple photographs taken from different angles to construct a digital three-dimensional model of the scanned object (Nauer et al., 2018b). To take photogrammetry measurements we first removed debris surrounding the mound and matted down any grass obscuring the mound. Starting at the north-facing side of the mound, consecutive photos were taken on an Apple iPad Pro (Cupertino, California, United States) as the person scanning walked clockwise around the mound, holding the iPad steady. The top of the mound was also

scanned when it was possible; on occasion this was constrained by mound height. Photos were digitally assembled in the Polycam app (Polycam Inc.) to create a three-dimensional photogrammetric termite mound model.

Individual mound models were exported as .glb files from Polycam app and imported into MeshLab to remove non-termite mound material using the selection tool (Cignoni et al., 2008). Total mound surface area was calculated in MeshLab using the *Compute Geometric Measures* function. To calculate total mound volume, cleaned mound models were imported into Blender as .obj files (Blender Online Community, 2018). Each mound was first filled with the *grid fill* command and volume was calculated using the 3D print toolbox *volume* function.

Mound wall thickness measurement

Mound wall thickness was recorded at the final measurement campaign (February 2024) due to the invasive nature of the measurement. After sampling CH_4 emissions, we used a drywall hammer or pickaxe (depending on mound hardness) to break the mound wall at each sampling point. We used digital calipers with 0.01 mm precision to record wall thickness, which was defined as the distance from the external wall to where termite galleries were visible.

Mound CH_4 emissions estimated at the landscape scale

We used data from Clement et al. (2021) which reports landscape abundance of occupied termite mounds per hectare for the three study species and at the Station Creek site. We calculated average annual mound CH_4 emission for each of our study species (Tg CH_4 yr^{-1} $mound^{-1}$) and then multiplied this value by mound density per hectare (Clement et al., 2021) to derive an estimate of landscape-scale termite mound emissions for northern Australian savanna ecosystems (Tg CH_4 yr^{-1} ha^{-1}). It is estimated that tropical savannas in northern Australia cover approximately 1.9 million km^2 (Chen et al., 2003), and termite mounds are characteristic features of this landscape, although it is noted that the proportion of dominant species may change for different locations in Australian tropical savannas.

Mound microbial community sampling and metagenomic sequencing

In May 2022 we sampled termite mound material to link microbial communities directly with CH_4 emissions. Following CH_4 emission measurement, the area covered by the chamber was broken to sample internal mound material (where termite galleries were) using a sterilized chisel and forceps. Mound substrate was placed into a 5 mL soil vial and subsequently frozen at -20°C.

We selected a subset of samples for microbial community analysis based on their suitability to address two questions: is microbial community variation associated with variation in CH_4 emission 1) between mounds and 2) within mounds? To test drivers of variation between mounds, for each of the three study species we selected the four mounds with the highest average CH_4 emission and the four with the lowest average CH_4 emission. For these mounds (n = 8 per species, n = 24 total mounds), we selected three subsamples within each mound that were closest to the average CH_4 emission for that mound for metagenomic sequencing (n = 72 total subsamples). To test drivers of variation within mounds, we first calculated the CH_4 emission range for each mound and then identified the five mounds with the highest variation for each species, indicated by the greatest CH_4 emission range. For these mounds we selected all subsamples (4 or 5) collected (n = 5 mounds per species, = 15 total mounds, n = 69 total subsamples). In total, we extracted DNA from and sequenced 115 mound samples, and there was overlap in which some samples were considered for both questions (i.e., a highly variable mound could also be a top-emitting mound).

DNA extractions were carried out with the DNeasy® PowerSoil® Pro Kit (Qiagen, United States) using the manufacturer's instructions with an input of approximately 250 mg mound material. Mound material was homogenized prior to extraction using a FastPrep-24™ 5G Homogenizer MP Biomedicals (MP Biomedicals, United States; settings: sediment - soils/rocks, Speed: 5.5 m sec^{-1}, Adapter: quickpro, Time: 30 s, Lysing matrix: E, Quantity: 50 mg, Cycles: 2, Pause time: 300 s). DNA concentration (ng μL^{-1}) and quality (260/280 and 260/230 values) were evaluated with a NanoDrop spectrophotometer (Thermo Fisher Scientific, Massachusetts, United States).

Metagenomic sequencing was performed at the Ramaciotti Centre for Genomics (UNSW, Sydney, Australia) on a NovaSeq X Plus 10B (2x150 bp; Illumina). Raw reads were first quality controlled using fastp v0.23.4 (Chen et al., 2018), then go reads error correction using the Bayesian-Hammer as implemented in SPAdes v4.0.0 (Prjibelski et al., 2020). Resultant corrected reads were assembled using Megahit v1.2.9 (Li et al., 2016); only contigs over 1 kb were retained for gene prediction. Parallelized version of Prodigal – pprodigal (Hyatt et al., 2010; Jaenicke 2022) was used for gene prediction; non-redundant genes (protein translations) were generated using CD-HIT v4.8.1 (Li & Godzik 2006), with parameters setting as -c 0.9 -M 0 -T 0 -l 20 -G 0 -aS 0.9 -g 0. KEGG Orthology (KO) and pathway analysis was performed using KofamKOALA (Aramaki et al., 2019, KofamScan v1.3.0 with the latest KOfam database v2024-08-29). Resultant tables (reads count per sample) including KO and pathway analysis were generated using CoverM (Aroney et al., 2024).

Identifying methanotrophic microbes and genes from metagenomic sequencing

From the metagenomic analyses described above, we targeted the *pmoA* gene as it plays a direct role in CH_4 metabolism (Zhou et al., 2015) and has been previously associated with termite mound CH_4 oxidation (Chiri

et al., 2020). We removed five samples with low total read counts (<300 reads) compared to the average read count across the dataset (mean = 18,762,769 reads). To account for variation in sequencing depth, we then resampled reads for the *pmoA* gene (KO number 'K10944') to standardize total reads to the minimum value of the dataset (6,913,446 reads). We calculated the relative abundance of the *pmoA* gene to use in subsequent analyses.

We identified methanotrophic bacterial genera from various literature sources and then queried our metagenomic sequencing data outputs for these 16 genera (Supplementary Table 11). From this list, 10 methanotroph genera were present in our mound samples. Regarding methanotrophic archaea, these genera are less well described in comparison to bacteria, although the *Candidatus methanoperedens* genus is known to be associated with methanotrophy (Bhattarai et al., 2019). However, we did not detect any methanotrophic members in the archaea metagenomic dataset, and therefore focused our analyses on the bacterial methanotroph community composition at the genus level.

Analyses

CH_4 emissions at the individual termite and mound-level

We used Analysis of Variance (ANOVA) to evaluate differences in TEFs of the three termite species. We used the R package *emmeans* (Lenth 2025) to perform pairwise species comparisons with Tukey's HSD adjustment for multiple testing. To evaluate differences among species in termite mound CH_4 emission, we used a linear mixed effect model from the R package *lmer* (Bates et al., 2015). In the model, CH_4 emission was the response, species was a fixed effect, and mound individual was included as a random effect to account for multiple measurements for each mound. In a post hoc analysis we compared estimated marginal means among species using Tukey's HSD adjustment for multiple comparisons.

Influence of species-specific mound structural traits and environmental drivers on mound-level CH_4 emission

We used piecewise Structural Equation Modeling (SEM) to explore the direct and indirect drivers of mound-level CH_4 emission from termite mounds. Specifically, we modeled how mound volume and wall thickness mediated the relationship between termite species and CH_4 flux, while also accounting for temperature and season effects. The SEM was built using the following three equations: 1) Mound volume (V) as a function of species (SP) in a linear model, 2) Wall thickness (W) as a function of species in a linear model, and 3) Mean CH_4 emission (E) as a function of all predictors (wall thickness (W), volume (V), species (SP), temperature (T), and season (S)) in a random effects model with individual mound as the random effect:

(1) $V = \beta_{0,V} + \beta_{1,V} * SP + \varepsilon_V$

(2) $W = \beta_{0,W} + \beta_{1,W} * SP + \varepsilon_W$

(3) $E = \beta_{0,E} + (\beta_{1,E} * V) + (\beta_{2,E} * W) + (\beta_{3,E} * SP) + (\beta_{4,E} * T) + (\beta_{5,E} * S) + \varepsilon_E$

Where $\beta_{0,x}$ is the model intercept for a given predictor variable (x), β_x is the slope of each predictor variable, and ε_y is the error of the response variable (y). In this analysis, mound volume and wall thickness predictors were scaled (mean-centered and divided by standard deviation).

The SEM was built using the *psem* function from the *piecewiseSEM* R package (Lefcheck 2016). We assessed model fit using the Fisher's C statistic and directed separation tests were used to verify that there were no important missing paths. Individual component models in the SEM were evaluated using standardized coefficients, confidence intervals, and p-values.

Mound methanotroph communities, genes, and influence on CH_4 emission: variation between mounds

For the subset of metagenomic data that captured variation between mounds, we explored patterns in the composition of methanotroph genera within termite mounds using a Principal Coordinates Analysis (PCoA). The analysis was based on a Bray-Curtis dissimilarity matrix of the mound methanotroph community and used the *wcmdscale* function from the *vegan* R package (Oksanen et al., 2025) with 2 dimensions (k = 2). We calculated weighted genera scores, and the resulting PCoA1 and PCoA2 scores were used to explore relationships between methanotroph community structure, termite species, and variation in CH_4 emission.

We then tested if methanotroph communities were predicted by termite species or by CH_4 emission using permutational multivariate analysis of variance (PERMANOVA) with the *adonis2* function (Oksanen et al., 2025), including 999 permutations to assess significance. Then, we used a linear mixed effect model to determine the relationship between methanotroph communities (summarized by PCoA1 and PCoA2 scores) and the relative abundance of the *pmoA* gene. In the model, PCoA1, PCoA2 and their interaction were predictors, and *pmoA* relative abundance was the response. Termite mound individual was included as a random effect.

Finally, we used a linear mixed effect model to determine if methanotroph community and gene predictors influenced CH_4 emission. Model predictors included the relative abundance of the *pmoA* gene, termite

mound species, the interaction between PCoA1 and PCoA2 scores, and the sum of all methanotroph genera relative abundances. Mound individual was included as a random effect. To explore this same relationship for each individual methanotroph genus, we ran separate models for each genus where the relative abundance of an individual methanotroph genus and termite mound species were predictors, CH_4 emission was the response, and mound individual was a random effect.

Mound methanotroph communities, genes, and influence on CH_4 emission: variation within mounds

For the subset of metagenomic data that captured variation within mounds, we carried out the same PCoA as described above to test PCoA1 and PCoA2 scores (including their interaction) as well as relative abundance of the *pmoA* gene, termite mound species, and the relative abundance of the sum of all methanotroph genera as predictors of CH_4 emission. Mound individual was included as a random effect. All analyses were conducted in R version 4.3.2.

Results

Scaling CH_4 emissions from individual termite- to mound- to landscape-levels

TEF values for individual termites (μg CH_4 g^{-1} termite h^{-1}) varied significantly by species ($F_{(2, 12)} = 29.41$, $p < 0.001$) with *C. acinaciformis* (mean TEF = 1.07) having a higher TEF than *A. laurensis* (mean TEF = 0.73), which had a higher TEF than *N. magnus* (mean TEF = 0.37). All pairwise comparisons were significant (Figure 2a, Supplementary Table 3). Average CH_4 emissions from termite mounds also significantly varied by species ($F_{(2, 125)} = 16.74$, $p < 0.001$) where *N. magnus* (3,426 μg CH_4 h^{-1} m^{-2}) had significantly greater emissions than both *A. laurensis* (1,270 μg CH_4 h^{-1} m^{-2}) and *C. acinaciformis* (1,323 μg CH_4 h^{-1} m^{-2}) but the latter two species did not significantly differ from one another (Figure 2b, Supplementary Table 4).

At the landscape scale, we estimated a combined annual emission of 2×10^{-9} Tg CH_4 ha^{-1} y^{-1} from termite mounds of our three study species (Supplementary Table 5). *Amitermes laurensis* contributed the most CH_4 on a per hectare basis (Figure 2c, mean = 1.04×10^{-9} Tg CH_4 ha^{-1} yr^{-1}), *N. magnus* was the second highest CH_4 emitter (Figure 2c, mean = 8.17×10^{-10} Tg CH_4 ha^{-1} yr^{-1}), while *C. acinaciformis* (Figure 2c, mean = 1.69×10^{-10} Tg CH_4 ha^{-1} yr^{-1}) contributed the least to landscape mound CH_4 emissions.

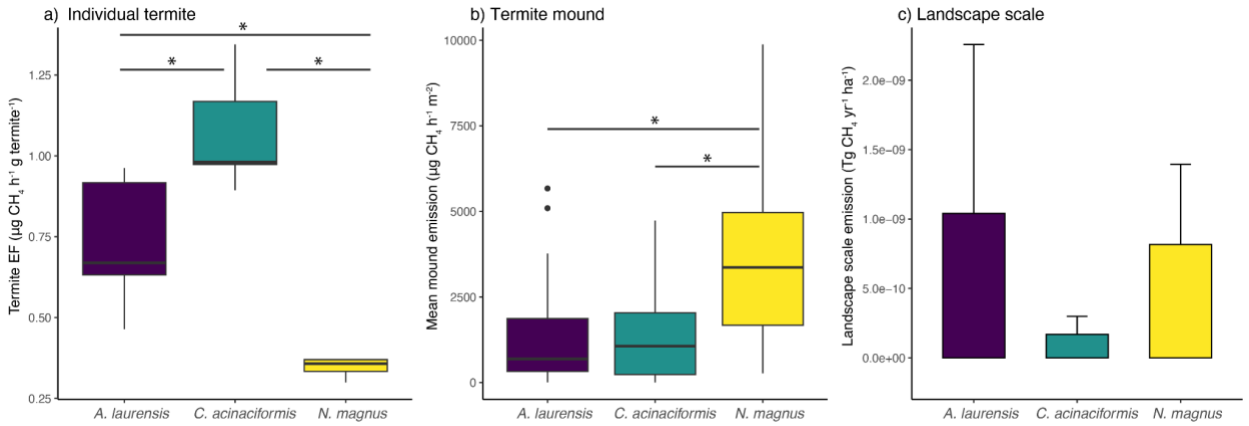

Figure 2. a) Termite emission factors (µg CH_4 h^{-1} g $termite^{-1}$) for the study species (purple = *A. laurensis*, green = *C. acinaciformis*, yellow = *N. magnus*). b) Average mound-level CH_4 emission (µg CH_4 h^{-1} m^{-2}) for the three study species. Boxplot center lines indicate the median and whiskers show ± 1.5 IQR, and asterisks indicate significantly different pairwise contrasts. c) Bar plot of landscape-scale mound CH_4 emissions (Tg CH_4 yr^{-1} ha^{-1}) by species. Bar plot error bars indicate one standard deviation.

Relative importance of structural traits and environmental drivers in mound-level CH_4 emission

There was a good overall fit to the data (marginal $R^2 = 0.30$, conditional $R^2 = 0.68$) in the SEM analysis, indicating no significant missing pathways (Fisher's C = 8.372, df = 10, p = 0.593). Termite species had a marginally significant effect on mean CH_4 emissions (p = 0.064, Figure 3), and mounds constructed by *C. acinaciformis* (β = 2747.3, p < 0.01, Supplementary Table 6) and *N. magnus* (β =5027.0, p < 0.001, Supplementary Table 6) exhibited significantly higher CH_4 emissions than those built by *A. laurensis*. Higher mound surface temperatures were positively associated with increased emissions (β = 2808.2, p = 0.038, Figure 3, Supplementary Table 6). Season significantly influenced flux (p < 0.001, Figure 3), with CH_4 emissions peaking during the wet-to-dry transition season (β = 4443.2, p < 0.001, Supplementary Table 6).

In contrast, mound volume and wall thickness, while hypothesized mediators of species-level effects on CH_4 emission, were not significant predictors of CH_4 emission (volume: p = 0.72; wall thickness: p = 0.55, Figure 3). Neither volume nor wall thickness differed significantly among species (Supplementary Table 6).

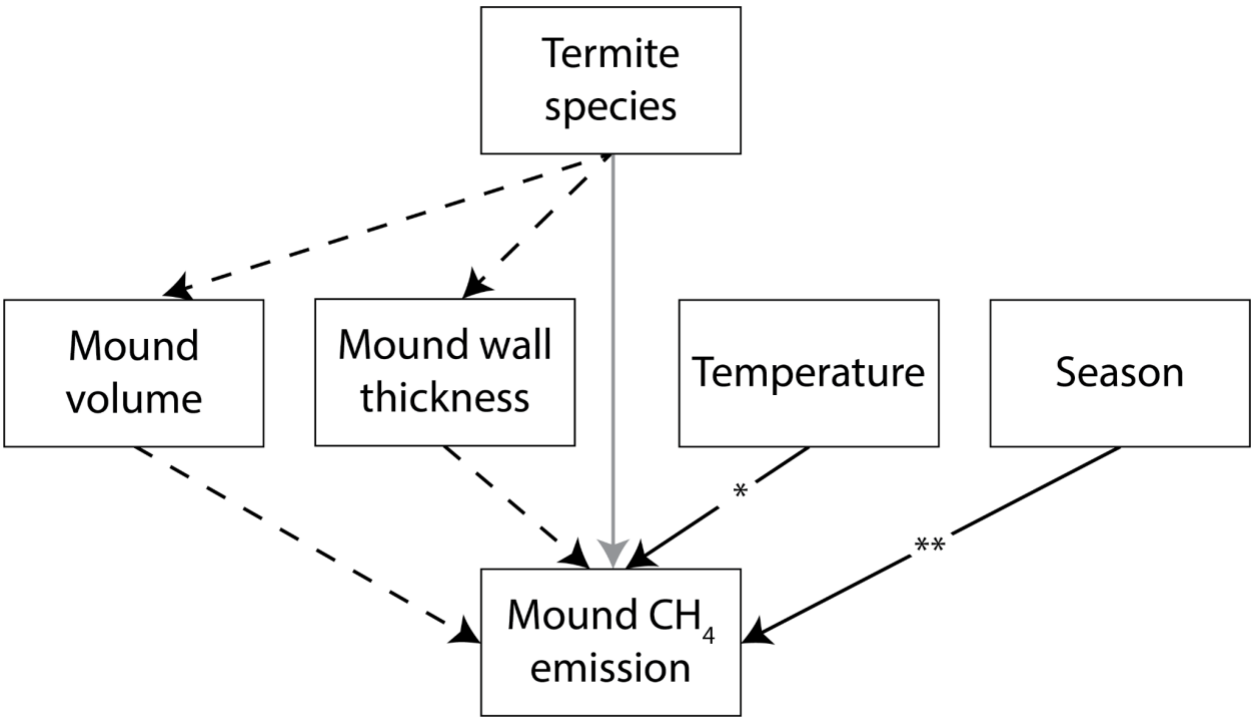

Figure 3. Structural equation modeling diagram showing significant (solid line with asterisk) and insignificant (dashed line) predictors of mound CH_4 emission. Grey solid lines, as shown between termite species and mound CH_4 emission, indicate a marginally significant relationship. Full SEM results are found in Supplementary Table 6.

Between mound variation in CH_4 emissions: bacterial methanotroph communities and the pmoA gene

Methanotrophic bacteria represented a small proportion of the bacterial community (0.25% of the total reads) and were dominated by *Methylocystis* sp. (Supplementary Figure 2). *Methylomicrobium, Methylobacter, Methylocaldum, Methylococcus* and *Methylomonas* were associated with high PCoA1 and PCoA2 values, which explained 36.9 and 5.2% of variation in the data, respectively. *Methylocapsa* was associated with low PCoA1 and high PCoA2 values, while the opposite was true for *Methylacidimicrobium*, *Methylosinus*, and *Methylocystis* genera. *Methylocella* was the only genera associated with low PCoA1 and PCoA2 values (Figure 4a).

Overall, there were poor links between bacterial methanotrophs and mound CH_4 emissions. Termite species explained only 1.5% of the variation in methanotroph communities (at the genus level, $R^2 = 0.015$, $F = 0.48$, $p = 0.73$) and CH_4 flux explained only 1.4% ($R^2 = 0.014$, $F = 0.90$, $p = 0.37$). There was minimal association between CH_4 emission and methanotroph community structure in terms of PCoA1 and PCoA2 (Figure 4a).

We found that *pmoA* gene relative abundance was negatively related to PCoA1 (β = -7.99, SE = 2.65, df = 55.11, t = -3.01, p = 0.004, Figure 4b) and not significantly related to PCoA2 scores (p = 0.65). However, there was a significant interaction between PCoA1 and PCoA2 (β = -343.33, SE = 154.88, df = 56.00, t = -2.22, p = 0.03, Figure 4b). At high values of PCoA2, there was a negative relationship between PCoA1 and *pmoA* gene relative abundance, while at low values of PCoA2, there was no significant relationship between PCoA1 and *pmoA* gene relative abundance.

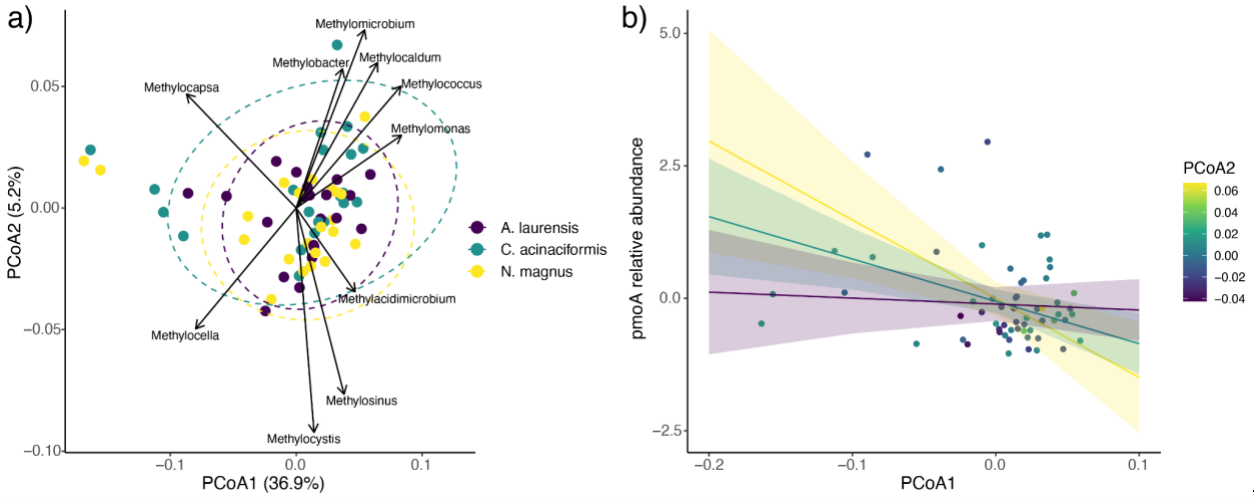

Figure 4. a) PCoA plot based on Bray Curtis dissimilarity for genera-level community composition of methanotrophs in mound material of the three termite study species (denoted by colored points and ellipses). Arrows indicate weighted genera vectors. b) A significant interaction between PCoA1 and PCoA2 predicting the relative abundance of the *pmoA* gene.

Finally, CH_4 emissions were not significantly predicted by relative abundance of *pmoA*, the sum of all methanotroph relative abundances, termite species, or PCoA1 and PCoA2 scores and their interaction (Supplementary Table 7). Additionally, the relative abundance of any single methanotroph bacterial genus was not significantly related to CH_4 emission (Supplementary Table 8).

Within mound variation in methane emissions: bacterial methanotroph communities and the pmoA gene

For those mounds with high intra-mound variation in CH_4 emissions, *N. magnus* mounds emitted marginally more CH_4 than *A. laurensis* mounds (β = 3420.91, SE = 1533.97, df = 11.32, t = 2.23, p = 0.047), but no other predictors (relative abundance of *pmoA*, sum of all methanotroph relative abundances, PCoA1 and PCoA2 and their interaction) were significant (Supplementary Table 9).

Discussion

In this study we sought to understand how the context of the termite mound environment shaped CH_4 emission by measuring the influence of species-level differences at various spatial scales, mound structural traits, environmental drivers, and methanotroph communities. We showed that the termite species with the highest TEFs were not the same species that emitted the most CH_4 across the mound surface and landscape level. Given that most CH_4 is likely emitted by termites inside mounds, accounting for the mound environment should be a critical consideration in calculating net CH_4 emission. Factors controlling termite mound emissions are therefore an important piece in accurately predicting termite contributions to the CH_4 budget. From our work, mound CH_4 emissions were most strongly influenced by termite species inhabiting the mounds and external environmental factors. Furthermore, while microbial methanotrophy within the mound has been shown to be an important filter controlling net CH_4 release, we did not find direct associations between either the bacterial methanotroph communities or the *pmoA* gene abundances and CH_4 release. However, the relationship between methanotroph communities and the *pmoA* gene suggests that expression, rather than relative abundance, may better reveal the interplay between termite methanogenesis, bacterial methanotrophy, and net mound CH_4 emission. Below we further explore the findings of this field study and discuss how incorporating considerations of scale, species-level differences, environmental factors, and methanotrophic microbes into CH_4 modeling can contribute to accurately estimating termites' role in global CH_4 budgets.

Species contributions to CH_4 emissions differ depending on the scale of measurement

The question of scale matters for determining the relative role of different termite species contributing to CH_4 emission. *Coptotermes acinaciformis* individuals had highest TEF values, *N. magnus* had highest mound-level emissions, and when mound density was factored into CH_4 emission calculations at the landscape-level, *A. laurensis* mounds had highest total emissions. At the individual scale, variation between species is most likely underpinned by differences in termite feeding habits and the gut microbial community that each species harbors (Clement 2022). While we were not able to directly test the effect of diet on CH_4 emission, there are known differences in how CH_4 varies by feeding group (Sanderson 1996; Zhou et al., 2022), which is ultimately controlled by termite gut microbial composition, specifically the presence and abundance of methanogenic microbes (Rouland et al., 1993). Interestingly, *Coptotermes acinaciformis*, which had the highest TEF in our study (contrasting Sanderson 1996 findings on wood-feeders), also had the greatest abundance of an archaeal methanogenic gut microbe (*Methanobrevibacter sp.*) compared to the other species in our study (Clement 2022). This link confirms the importance of understanding the balance of methanogenesis and methanotrophy occurring within termites and the termite mound, as even with high CH_4 production for *C. acinaciformis* individuals, *C. acinaciformis* mounds were significantly lower contributors to CH_4 emissions.

Differences in top emitting species at the mound and landscape scale were underpinned by tradeoffs between high average emissions and high landscape level termite mound densities. *Nasutitermes magnus* mounds were larger (mean surface area = 4.5 m^2) and had an average mound emission (3,426 μg CH_4 h^{-1} m^{-2}) that was greater than *A. laurensis* (1,270 μg CH_4 h^{-1} m^{-2}). However, *A. laurensis* mounds, although they were smaller (mean surface area = 0.7 m^2) were approximately 22 times more abundant compared to *N. magnus* mounds per hectare, leading to a greater overall contribution by *A. laurenesis* when CH_4 was estimated per hectare per year ($1.04 \times 10^{-9} > 8.17 \times 10^{-10}$ Tg CH_4 ha^{-1} yr^{-1}). Taken together, we propose that combining whole-mound CH_4 measurements with landscape-scale mound density to calculate a 'mound emission factor' per area provides more accurate representation of ecosystem CH_4 emission than using the commonly applied TEF (Saunois et al., 2020; Ito, 2023), especially in tropical savannas and other ecosystems with high mound abundance.

Temperature and season impact CH_4 emission more than mound architecture

The differences in CH_4 emissions that we found at various scales of measurement (individual, mound, landscape) also emphasize the importance of the 'colony context'. Methane emissions from termites should largely be released from the workers when they are inside termite mounds. Thus, net CH_4 emissions are not only shaped by production from gut methanogens within termites (Brune & Dietrich 2015), but also by the physical (mound structure and microbes) and external environment (temperature and seasonality) in which the termite lives (Korb 2003; Singh et al., 2019; Nauer et al., 2018a; Jamali et al., 2011b). In our system, temperature and season emerged as strong predictors of CH_4 emission contributing to the growing body of literature suggesting termites and termite driven decomposition are highly sensitive to environmental conditions (Zanne et al., 2022, Law et al., 2024b). Importantly, these external environments were more influential than the mound structure traits that we measured (wall thickness and volume). While not considered in the present study, the diffusion of gases such as CH_4 through the mound could relate to mound material permeability and porosity (Singh et al., 2019); it was shown that *C. acinaciformis* mound material was both harder and denser compared to the to the other study species (Clement et al., unpublished data), which could limit the movement of gas such as CH_4. These other variables, which may be more indicative of gas diffusion, could explain why *C. acinaciformis* individuals emitted high amounts of CH_4 yet average *C. acinaciformis* mound emissions were so low.

Interestingly, our results revealed far less seasonal variation in mound CH_4 emissions compared to previous studies. One study in northern Australia reported up to 26-fold higher emissions in the wet compared to the dry season for *Microcerotermes nervosus* mounds (Jamali et al., 2011a) and another study in Africa showed

549 contrasting findings, where wet season emissions were 64% lower than the dry season (Räsänen et al.,
550 2023). However, while we found that CH_4 emissions in the wet-to-dry transition season were significantly
551 greater than the mid-wet and dry-to-wet seasons, they were not drastically higher (33% and 28% higher,
552 respectively). Notably, our wet season CH_4 measurements took place following Cyclone Jasper, which
553 caused flooding at the site. It is possible that this anomalous inundation altered seasonal termite population
554 dynamics and concealed some of extreme wet season dynamics in CH_4 emission that were observed by
555 Jamali et al. (2011b). However, the significant effect of seasonal change that we observed could be
556 attributed to numerous factors, such as the fluctuation of termite mound population with alterations to water
557 and food resources (Jamali et al., 2011b), as well as interactions between temperature and moisture
558 availability on the metabolic functioning of both termites and microbes.
559
560 As temperatures increased so too did mound CH_4 emission, pointing to climatic regulation of termite
561 metabolic activity (Jamali et al., 2011b; Zanne et al., 2022), as well as the methanogenic microbes in termite
562 guts. Establishing such relationships between temperature and CH_4 emissions can be a critical advancement
563 in developing biogeochemical cycling models to predict how termite mound contributions to savanna and
564 global scale CH_4 emissions under future climate conditions (Zanne et al., 2022). Our results are especially
565 relevant as studies project that termite-mediated decomposition rates respond positively to increased
566 temperatures (Zanne et al., 2022), and termite range expansion is another predicted consequence of climate
567 warming (Zanne et al., 2022; Ito 2023). Ito (2023) estimated that from elevated CO_2 (via vegetation
568 productivity), climatic warming, and land-use change, termite CH_4 emissions could increase between 0.5-
569 5.9 Tg yr^{-1}. Given that our study provides species-specific, field-based measurements to define a
570 temperature-emission relationship, these could serve as a foundation to evaluate the validity of such claims.
571
572 Additionally, when predicting if emissions will increase due to higher temperatures and range expansion,
573 it is necessary to consider which termite species will expand in range, and what nesting behaviors they have
574 (Law et al., 2024a). Increases in subterranean-dwelling termites are unlikely to affect net CH_4 emission as
575 soils oxidize most of the termite-released CH_4 (Eggleton et al., 1999). Mound-building species are better
576 adapted to warmer temperatures because they can maintain internal homeostasis (Korb 2011; Wijas et al.,
577 2022). This could allow mound-building species to increase their ranges with climate warming, resulting
578 in additional termite CH_4 emissions as they decompose plant materials the expanded area. To predict such
579 changes in termite CH_4 under future climates, a step forward would be to modify existing ecosystem models
580 to include parameters for termites, including termite CH_4 generation, range expansion, and microbial
581 oxidation occurring within the mound (Law et al., 2024a). For one northern Australian termite species
582 (*Microcerotermes* sp.), Law et al. (2024a) showed that CH_4 production decreased above 35°C, suggesting

that there may be an upper limit for which the positive relationship between temperature and emission holds true. Above this value, it is possible that termites and termite-associated microbial functions may decline, thus diminishing CH_4 emissions. Given that in our study we measured three (but dominant in our system) species of termites, we provide a small insight as to how termite CH_4 emissions can respond to changing temperatures. Moving forward, the relationship we describe between termite mound CH_4 emission and temperature should be tested in other systems and across a range of species. With this, we can establish a growing database of termite contributions to the global CH_4 budget while parameterizing different influences of the mound environment.

The influence of mound methanotroph communities on functional genes, but not CH_4 emission

In our analysis of metagenomic data from termite mound material we found that specific combinations of the bacterial methanotroph community (represented by PCoA1 and PCoA2 scores) jointly determined the response of CH_4 emission. Interestingly, methanotrophs were rare members of the mound bacterial community (0.25% of all genera), which is in accordance with results reported by Chiri et al. (2020). Of the 16 methanotrophic bacterial genera that we identified, 10 genera were found in the termite mound material we sampled, suggesting that termite mounds harbor a diverse methanotroph community. While we showed no species-level differences in methanotrophic members in mound material, future work to characterize methanotrophs found in the mounds of other species in other places would help to determine if the methanotroph communities assembling in termite mounds are broadly consistent.

Surprisingly, we were unable to directly link local methanotroph communities or *pmoA* gene abundance to lower CH_4 emission. In contrast, Nauer et al. (2018a) showed that 50% of termite-produced CH_4 was oxidized on average prior to leaving the mound for three North Australian termite species (*Microcerotermes nervosus*, *Macrognathotermes sunteri*, and *Tumulitermes pastinator*), suggesting that mound methanotrophs play an important role in net CH_4 release. It appears that the missing link between methanotrophy potential, as indicated by relative abundances, and the result of CH_4 oxidation in termite mounds is an understanding of *pmoA* expression. Metatranscriptomics could be used to better identify the direct function of bacterial methanotrophy and its subsequent impacts on CH_4 emission. Future studies should pursue a more integrated approach with field CH_4 measurements and microbial ecology, using both metagenomics and metatranscriptomics to determine functional and community-based methanotrophic controls on net CH_4 emission from termite mounds. Lastly, mapping methanotroph-associated gene expression across a range of environmental conditions, especially temperature, would provide insight as to the temporal and climate-mediated shifts in methanotrophy within the mound.

What is the most effective way to upscale CH_4 emissions from termite mounds?

As an alternative to the TEF and biomass approach, mound-level CH_4 emission factors may have greater utility. Emissions at the mound-level have been recorded for a growing number of species across tropical ecosystems (Supplementary Table 10), and while not as robustly characterized as TEFs (Zhou et al., 2022), collecting CH_4 emission data across the diversity of mound-building termites is a key research objective for improving global estimates (Law et al., 2024a). Additionally, given the variability in termite mound sizes, it is useful to pair mound-level emission factors with average mound sizes. Photogrammetry is an accessible tool for this, as it is a portable method utilizing a simple smartphone app and a small amount of post-processing which can be done in open-source programs (i.e., Polycam, MeshLab, Blender).

Even with a broad database of mound-level emission factors, there remains the challenge of determining landscape-level mound abundance (Law et al., 2024a). Termite mounds range in spatial distribution, demonstrating both aggregated and more evenly distributed patterns (Davies et al., 2014; Levick et al., 2010), making field surveys challenging. Technologies such as airborne Lidar allows for epigeal mounds to be detected and mapped over large areas with greater ease (Levick et al., 2010; D'hont et al., 2021) and could be used to quantify mound dimensions (i.e., height and volume, D'hont et al., 2021). Paired with broader characterization of mound-level CH_4 emission across the termite diversity of a given region, remotely sensed termite mound abundance data will substantially reduce uncertainty in CH_4 accounting efforts.

Conclusion

Our findings highlight both the complexity and the opportunity in refining global termite CH_4 emissions by incorporating the context and dynamics of the termite mound environment. Termite species, temperature, and season emerge as important factors that should be used to improve estimates of global termite CH_4 emissions. Future research directly linking methanotrophy-associated gene expression in microbes within mounds to CH_4 oxidation could help define a microbial oxidation factor applicable to mound CH_4 emissions on a larger scale. Additionally, measuring mound-level emission factors for the global diversity of mound-building species can incorporate microbial oxidation and relieve errors inherent in calculations relying only on TEFs and termite biomass. Our understanding of the factors influencing termite mound methane in Australian savannas can be used to refine termite contributions to the global CH_4 budget.

Author Contributions

Conceptualization: Abbey R. Yatsko, Amy E. Zanne

Data collection: Abbey R. Yatsko, Caleb Jones, Baptiste Wijas

Data analysis: Abbey R. Yatsko, Paul Eggleton, Marcos Pérez-Losada, Jeff R. Powell, Ignacio Ramos-Tapia, Baptiste Wijas

Writing: Abbey R. Yatsko

Editing and review: all authors

Acknowledgements

The authors would like to thank the station managers at the Brooklyn Sanctuary, Kerri and Gavin Enever, for support in the field, and to the Australian Wildlife Conservancy for allowing us to collect data on their property. We thank Lucas Cernusak for allowing us to use laboratory space at James Cook University Cairns for the duration of this project. We also thank Alex Cheesman for assistance with organizing fieldwork logistics, and Steve Allison for funding support (US National Science Foundation, Ecosystem Studies Cluster, DEB-1655340). Jiayu Li provided essential help with metagenomic data analysis, and Juntao Wang assisted with data transfer and server support. We thank Michelle Afkhami for feedback on the manuscript and metagenomic analyses, as well as Michael Bewley-Green, Allyson Malpartida and Lily Dun for helping to collect field data.

Funding Information

This work was supported by the University of Miami Biology Department and a National Science Foundation Graduate Research Fellowship (Award #1938060) to ARY. Funding was also acquired from the US National Science Foundation, Ecosystem Studies Cluster, under awards DEB-1655759 and DEB-2149151 to AEZ as well as a UK NERC grant NE/K01613X/1 to PE.

References

Aramaki, T., Blanc-Mathieu, R., Endo, H., Ohkubo, K., Kanehisa, M., Goto, S., & Ogata, H. (2020). KofamKOALA: KEGG Ortholog assignment based on profile HMM and adaptive score threshold. *Bioinformatics*, *36*(7), 2251–2252. https://doi.org/10.1093/bioinformatics/btz859

Aroney, S. T. N., Newell, R. J. P., Nissen, J., Camargo, A. P., Tyson, G. W., & Woodcroft, B. J. (2024). CoverM: Read coverage calculator for metagenomics (v0.7.0). Zenodo. https://doi.org/10.5281/zenodo.10531254

Arora, J., Kinjo, Y., Šobotník, J., Buček, A., Clitheroe, C., Stiblik, P., Roisin, Y., Žifčáková, L., Park, Y. C., Kim, K. Y., Sillam-Dussès, D., Hervé, V., Lo, N., Tokuda, G., Brune, A., & Bourguignon, T. (2022). The functional evolution of termite gut microbiota. *Microbiome*, *10*(1), 78. https://doi.org/10.1186/s40168-022-01258-3

Awala, S. I., Gwak, J. H., Kim, Y., Seo, C., Strazzulli, A., Kim, S. G., & Rhee, S. K. (2023). Methylacidiphilum caldifontis gen. Nov., sp. Nov., a thermoacidophilic methane-oxidizing bacterium from an acidic geothermal environment, and descriptions of the family Methylacidiphilaceae fam. Nov. And order Methylacidiphilales ord. Nov. International Journal of Systematic and Evolutionary Microbiology, 73(10), 006085. https://doi.org/10.1099/ijsem.0.006085

Bates, D., Mächler, M., Bolker, B., & Walker, S. (2015). Fitting Linear Mixed-Effects Models Using lme4. Journal of Statistical Software, 67, 1–48. https://doi.org/10.18637/jss.v067.i01

Bhattarai, S., Cassarini, C., & Lens, P. N. L. (2019). Physiology and Distribution of Archaeal Methanotrophs That Couple Anaerobic Oxidation of Methane with Sulfate Reduction. Microbiology and molecular biology reviews: MMBR, 83(3), e00074-18. https://doi.org/10.1128/MMBR.00074-18

Bowman, J.P. (2015). Methylosphaera. In Bergey's Manual of Systematics of Archaea and Bacteria (eds M.E. Trujillo, S. Dedysh, P. DeVos, B. Hedlund, P. Kämpfer, F.A. Rainey and W.B. Whitman). https://doi.org/10.1002/9781118960608.gbm01185

Bowman, J. P., Sly, L. I., Nichols, P. D., & Hayward, A. C. (1993). Revised Taxonomy of the Methanotrophs: Description of Methylobacter gen. nov., Emendation of Methylococcus, Validation of Methylosinus and Methylocystis Species, and a Proposal that the Family Methylococcaceae Includes Only the Group I Methanotrophs. International Journal of Systematic and Evolutionary Microbiology, 43(4), 735–753. https://doi.org/10.1099/00207713-43-4-735

Brümmer, C., Papen, H., Wassmann, R., & Brüggemann, N. (2009). Fluxes of CH4 and CO2 from soil and termite mounds in south Sudanian savanna of Burkina Faso (West Africa). *Global Biogeochemical Cycles*, *23*(1), 2008GB003237. https://doi.org/10.1029/2008GB003237

Brune, A., & Dietrich, C. (2015). The Gut Microbiota of Termites: Digesting the Diversity in the Light of Ecology and Evolution. *Annual Review of Microbiology*, *69*(1), 145–166. https://doi.org/10.1146/annurev-micro-092412-155715

Bunney, K., Robertson, M., Eggleton, P., Twine, W., & Parr, C. (2024). Quantifying the role of termite decomposition in a mesic savanna. *Biotropica*, *56*(4), e13333. https://doi.org/10.1111/btp.13333

Chen, S., Zhou, Y., Chen, Y., & Gu, J. (2018). fastp: An ultra-fast all-in-one FASTQ preprocessor. *Bioinformatics*, *34*(17), i884–i890. https://doi.org/10.1093/bioinformatics/bty560

Chen, X., Hutley, L. B., & Eamus, D. (2003). Carbon balance of a tropical savanna of northern Australia. Oecologia, 137(3), 405–416. https://www.jstor.org/stable/4223778.

Chiri, E., Greening, C., Lappan, R., Waite, D. W., Jirapanjawat, T., Dong, X., Arndt, S. K., & Nauer, P. A. (2020). Termite mounds contain soil-derived methanotroph communities kinetically

adapted to elevated methane concentrations. *ISME Journal*, *14*(11), 2715–2731. https://doi.org/10.1038/s41396-020-0722-3

Clement, R. A., Flores-Moreno, H., Cernusak, L. A., Cheesman, A. W., Yatsko, A. R., Allison, S. D., Eggleton, P., & Zanne, A. E. (2021). Assessing the Australian Termite Diversity Anomaly: How Habitat and Rainfall Affect Termite Assemblages. *Frontiers in Ecology and Evolution*, *9*, 657444. https://doi.org/10.3389/fevo.2021.657444

Clement, R. A. (2022). Australian Termite Diversity [Doctoral dissertation, The George Washington University]. ProQuest Dissertations & Theses. https://www.proquest.com/openview/d03271101407d3de06ef157eef6ab359/1?pq-origsite=gscholar&cbl=18750&diss=y

Cupples, A. M., & Thelusmond, J.-R. (2022). Predicting the occurrence of monooxygenases and their associated phylotypes in soil microcosms. *Journal of Microbiological Methods*, *193*, 106401. https://doi.org/10.1016/j.mimet.2021.106401

Davies, A. B., Levick, S. R., Asner, G. P., Robertson, M. P., van Rensburg, B. J., & Parr, C. L. (2014). Spatial variability and abiotic determinants of termite mounds throughout a savanna catchment. *Ecography*, *37*(9), 852–862. https://doi.org/10.1111/ecog.00532

Delherbe, N. A., Pearce, D., But, S. Y., Murrell, J. C., Khmelenina, V. N., & Kalyuzhnaya, M. G. (2024). Genomic Insights into Moderately Thermophilic Methanotrophs of the Genus *Methylocaldum*. *Microorganisms*, 12(3), 469. https://doi.org/10.3390/microorganisms12030469

D'hont, B., Calders, K., Bartholomeus, H., Whiteside, T., Bartolo, R., Levick, S., Moorthy, S. M. K., Terryn, L., & Verbeeck, H. (2021). Characterising termite mounds in a tropical savanna with UAV laser scanning. *Remote Sensing*, *13*(3), 1–19. https://doi.org/10.3390/rs13030476

Dunfield, P. F. (2007). The soil methane sink. In *Greenhouse gas sinks* (pp. 152–170). https://doi.org/10.1079/9781845931896.0152

Dunfield, P. F., Belova, S. E., Vorob'ev, A. V., Cornish, S. L., & Dedysh, S. N. (2010). Methylocapsa aurea sp. Nov., a facultative methanotroph possessing a particulate methane monooxygenase, and emended description of the genus Methylocapsa. International Journal of Systematic and Evolutionary Microbiology, 60(11), 2659–2664. https://doi.org/10.1099/ijs.0.020149-0

Dunfield, P.F. (2016). Methylohalobius†,‡. In Bergey's Manual of Systematics of Archaea and Bacteria (eds M.E. Trujillo, S. Dedysh, P. DeVos, B. Hedlund, P. Kämpfer, F.A. Rainey and W.B. Whitman). https://doi.org/10.1002/9781118960608.gbm01418

Eggleton, P., Homathevi, R., Jones, D. T., MacDonald, J. A., Jeeva, D., Bignell, D. E., Davies, R. G., & Maryati, M. (1999). Termite assemblages, forest disturbance and greenhouse gas fluxes in

751 Sabah, East Malaysia. *Philosophical Transactions of the Royal Society B*, *354*(1391), 1791–1802.
752 https://doi.org/10.1098/rstb.1999.0521
753 Flores-Moreno, H., Yatsko, A. R., Cheesman, A. W., Allison, S. D., Cernusak, L. A., Cheney, R.,
754 Clement, R. A., Cooper, W., Eggleton, P., Jensen, R., Rosenfield, M., & Zanne, A. E. (2024).
755 Shifts in internal stem damage along a tropical precipitation gradient and implications for forest
756 biomass estimation. The New Phytologist, 241(3), 1047–1061.
757 https://doi.org/10.1111/nph.19417
758 Griffiths, H. M., Ashton, L. A., Evans, T. A., Parr, C. L., & Eggleton, P. (2019). Termites can
759 decompose more than half of deadwood in tropical rainforest. *Current Biology*, *29*(4), R118–
760 R119. https://doi.org/10.1016/j.cub.2019.01.012
761 Ho, A., Erens, H., Mujinya, B. B., Boeckx, P., Baert, G., Schneider, B., Frenzel, P., Boon, N., & van
762 Ranst, E. V. (2013). Termites facilitate methane oxidation and shape the methanotrophic
763 community. *Applied and Environmental Microbiology*, *79*(23), 7234–7240.
764 https://doi.org/10.1128/AEM.02785-13
765 Holdo, Ricardo & McDowell, Lee. (2004). Termite Mounds as Nutrient–Rich Food Patches for
766 Elephants. *Biotropica*. 36. 231 - 239. 10.1111/j.1744-7429.2004.tb00314.x.
767 Houghton, K. M., Carere, C. R., Stott, M. B., & McDonald, I. R. (2019). Thermophilic methanotrophs:
768 In hot pursuit. *FEMS Microbiology Ecology*, 95(9), fiz125. https://doi.org/10.1093/femsec/fiz125
769 Hyatt, D., Chen, G. L., LoCascio, P. F. Land, M. L., Larimer F. W. & Hauser L. J. (2010). Prodigal:
770 prokaryotic gene recognition and translation initiation site identification. *BMC Bioinformatics,*
771 11(119). https://doi.org/10.1186/1471-2105-11-119
772 IPCC, 2021: Climate Change 2021: The Physical Science Basis. Contribution of Working Group I to
773 the Sixth Assessment Report of the Intergovernmental Panel on Climate Change [Masson-
774 Delmotte, V., P. Zhai, A. Pirani, S.L. Connors, C. Péan, S. Berger, N. Caud, Y. Chen, L. Goldfarb,
775 M.I. Gomis, M. Huang, K. Leitzell, E. Lonnoy, J.B.R. Matthews, T.K. Maycock, T. Waterfield,
776 O. Yelekçi, R. Yu, and B. Zhou (eds.)]. Cambridge University Press, Cambridge, United
777 Kingdom and New York, NY, USA, In press, doi:10.1017/9781009157896.
778 Ito, A. (2023). Global termite methane emissions have been affected by climate and land-use changes.
779 *Scientific Reports*, *13*(1), 17195. https://doi.org/10.1038/s41598-023-44529-1
780 Jaenicke, S. (2022). pprodigal - Python3 wrapper for parallelized gene prediction using Prodigal.
781 GitHub repository, https://github.com/sjaenick/pprodigal
782 Jamali, H., Livesley, S. J., Dawes, T. Z., Cook, G. D., Hutley, L. B., & Arndt, S. K. (2011a). Diurnal
783 and seasonal variations in CH_4 flux from termite mounds in tropical savannas of the Northern

Territory, Australia. *Agricultural and Forest Meteorology*, *151*(11), 1471–1479. https://doi.org/10.1016/j.agrformet.2010.06.009

Jamali, H., Livesley, S. J., Dawes, T. Z., Hutley, L. B., & Arndt, S. K. (2011b). Termite mound emissions of CH_4 and CO_2 are primarily determined by seasonal changes in termite biomass and behaviour. *Oecologia*, *167*(2), 525–534. https://doi.org/10.1007/s00442-011-1991-3

Jamali, H., Livesley, S. J., Grover, S. P., Dawes, T. Z., Hutley, L. B., Cook, G. D., & Arndt, S. K. (2011c). The Importance of Termites to the CH_4 Balance of a Tropical Savanna Woodland of Northern Australia. *Ecosystems*, *14*(5), 698–709. https://doi.org/10.1007/s10021-011-9439-5

Jeffrey, L. C., Maher, D. T., Tait, D. R., & Johnston, S. G. (2020). A Small Nimble In Situ Fine-Scale Flux Method for Measuring Tree Stem Greenhouse Gas Emissions and Processes (S.N.I.F.F). *Ecosystems*, *23*(8), 1676–1689. https://doi.org/10.1007/s10021-020-00496-6

Josens, G., & Soki, K. (2010). Relation between termite numbers and the size of their mounds. *Insectes Sociaux*, *57*(3), 303–316. https://doi.org/10.1007/s00040-010-0085-2

Jouquet, P., Guilleux, N., Shanbhag, R. R., & Subramanian, S. (2015). Influence of soil type on the properties of termite mound nests in Southern India. *Applied Soil Ecology*, *96*, 282–287. https://doi.org/10.1016/j.apsoil.2015.08.010

Kalyuzhnaya, M.G. (2016a). *Methylosarcina*. Bergey's Manual of Systematics of Archaea and Bacteria (eds W.B. Whitman, F. Rainey, P. Kämpfer, M. Trujillo, J. Chun, P. DeVos, B. Hedlund and S. Dedysh). https://doi.org/10.1002/9781118960608.gbm01184.pub2

Kalyuzhnaya, M.G. (2016b). *Methylomicrobium*. In Bergey's Manual of Systematics of Archaea and Bacteria (eds W.B. Whitman, F. Rainey, P. Kämpfer, M. Trujillo, J. Chun, P. DeVos, B. Hedlund and S. Dedysh). https://doi.org/10.1002/9781118960608.gbm01182.pub2

Khalil, M., Rasmussen, R., French, J. R., & Holt, J. A. (1990). The Influence of Termites on Atmospheric Trace Gases: CH4, CO2, CHC13, N20, CO, H2, and Light Hydrocarbon. *Journal of Geophysical Research*, *95*, 3619–3634.

Kirschke, S., Bousquet, P., Ciais, P., Saunois, M., Canadell, J. G., Dlugokencky, E. J., Bergamaschi, P., Bergmann, D., Blake, D. R., Bruhwiler, L., Cameron-Smith, P., Castaldi, S., Chevallier, F., Feng, L., Fraser, A., Heimann, M., Hodson, E. L., Houweling, S., Josse, B., … Zeng, G. (2013). Three decades of global methane sources and sinks. *Nature Geoscience*, *6*(10), 813–823. https://doi.org/10.1038/ngeo1955

Korb, J. (2003). Thermoregulation and ventilation of termite mounds. *Die Naturwissenschaften*, *90*(5), 212–219. https://doi.org/10.1007/s00114-002-0401-4

Korb, J. (2011). Termite Mound Architecture, from Function to Construction. In D. E. Bignell, Y. Roisin, & N. Lo (Eds.), *Biology of Termites: A Modern Synthesis* (pp. 349–373). Springer Netherlands. https://doi.org/10.1007/978-90-481-3977-4_13

Law, S. J., Allison, S. D., Davies, A. B., Flores-Moreno, H., Wijas, B. J., Yatsko, A. R., Zhou, Y., Zanne, A. E., & Eggleton, P. (2024a). The challenge of estimating global termite methane emissions. *Global Change Biology*, *30*(6), e17390. https://doi.org/10.1111/gcb.17390

Law, S. J., Flores-Moreno, H., Parr, C. L., Adu-Bredu, S., Bunney, K., Cornwell, W. K., Evouna Ondo, F., Powell, J. R., Quansah, G. W., Robertson, M. P., Zanne, A. E., & Eggleton, P. (2024b). Biogeographical Variation in Termite Distributions Alters Global Deadwood Decay. *Global Ecology and Biogeography*, *33*(12), e13915. https://doi.org/10.1111/geb.13915

Lefcheck, J.S. (2016). piecewiseSEM: Piecewise structural equation modelling in R for ecology, evolution, and systematics. *Methods in Ecology and Evolution*, *7*, 573-579. https://doi.org/10.1111/2041-210X.12512

Lenth R. (2025). emmeans: Estimated Marginal Means, aka Least-Squares Means. R package version 1.11.1-00001, https://rvlenth.github.io/emmeans/.

Levick, S. R., Asner, G. P., Chadwick, O. A., Khomo, L. M., Rogers, K. H., Hartshorn, A. S., Kennedy-Bowdoin, T., & Knapp, D. E. (2010). Regional insight into savanna hydrogeomorphology from termite mounds. *Nature Communications*, *1*(1), 65. https://doi.org/10.1038/ncomms1066

Li, D., Luo, R., Liu, C.-M., Leung, C.-M., Ting, H.-F., Sadakane, K., Yamashita, H., & Lam, T.-W. (2016). MEGAHIT v1.0: A fast and scalable metagenome assembler driven by advanced methodologies and community practices. *Methods*, *102*, 3–11. https://doi.org/10.1016/j.ymeth.2016.02.020

Li, W., & Godzik, A. (2006). Cd-hit: A fast program for clustering and comparing large sets of protein or nucleotide sequences. *Bioinformatics*, *22*(13), 1658–1659. https://doi.org/10.1093/bioinformatics/btl158

Macdonald, J. A., Eggleton, P., Bignell, D. E., Forzi, F., & Fowler, D. (1998). Methane emission by termites and oxidation by soils, across a forest disturbance gradient in the Mbalmayo Forest Reserve, Cameroon. *Global Change Biology*, *4*(4), 409–418. https://doi.org/10.1046/j.1365-2486.1998.00163.x

Martius, C., Wassmann, R., Thein, U., Bandeira, A., Rennenberg, H., Junk, W., & Seiler, W. (1993). Methane emission from wood-feeding termites in Amazonia. *Chemosphere*, *26*(1), 623–632. https://doi.org/10.1016/0045-6535(93)90448-E

Meyer, V. W., Braack, L. E. O., Biggs, H. C., & Ebersohn, C. (1999). Distribution and density of termite mounds in the northern Kruger National Park, with specific reference to those constructed by Macrotermes Holmgren (Isoptera: Termitidae). *African Entomology*, *7*(1), 123–130.

Nauer, P. A., Hutley, L. B., & Arndt, S. K. (2018a). Termite mounds mitigate half of termite methane emissions. *Proceedings of the National Academy of Sciences*, *115*(52), 13306–13311. https://doi.org/10.1073/pnas.1809790115

Nauer, P. A., Chiri, E., De Souza, D., Hutley, L. B., & Arndt, S. K. (2018b). Technical note: Rapid image-based field methods improve the quantification of termite mound structures and greenhouse-gas fluxes. *Biogeosciences*, *15*(12), 3731–3742. https://doi.org/10.5194/bg-15-3731-2018

Neto, M. D. de A., Furley, P. A., Haridasan, M., & Johnson, C. E. (1986). The murundus of the cerrado region of Central Brazil. *Journal of Tropical Ecology*, *2*(1), 17–35. https://doi.org/10.1017/S0266467400000559

Ocko, S. A., Heyde, A., & Mahadevan, L. (2019). Morphogenesis of termite mounds. *Proceedings of the National Academy of Sciences*, *116*(9), 3379–3384. https://doi.org/10.1073/pnas.1818759116

Oksanen J, Simpson G, Blanchet F, Kindt R, Legendre P, Minchin P, O'Hara R, Solymos P, Stevens M, Szoecs E, Wagner H, Barbour M, Bedward M, Bolker B, Borcard D, Borman T, Carvalho G, Chirico M, De Caceres M, Durand S, Evangelista H, FitzJohn R, Friendly M, Furneaux B, Hannigan G, Hill M, Lahti L, Martino C, McGlinn D, Ouellette M, Ribeiro Cunha E, Smith T, Stier A, Ter Braak C, Weedon J (2025). vegan: Community Ecology Package. R package version 2.8-0, https://vegandevs.github.io/vegan/.

Prjibelski, A., Antipov, D., Meleshko, D., Lapidus, A., & Korobeynikov, A. (2020). Using SPAdes De Novo Assembler. *Current Protocols in Bioinformatics*, *70*(1), e102. https://doi.org/10.1002/cpbi.102

Quevedo, H. D., Brandani, C. B., Bento, C. B., Pitombo, L. M., Ferreira Filho, P. J., & Braga Do Carmo, J. (2021). Greenhouse gas emissions from termite mounds in a transition area between the Cerrado Savanna and the Atlantic Forest in Brazil. *Acta Oecologica*, *110*, 103690. https://doi.org/10.1016/j.actao.2020.103690

Räsänen, M., Vesala, R., Rönnholm, P., Arppe, L., Manninen, P., Jylhä, M., Rikkinen, J., Pellikka, P., & Rinne, J. (2023). Carbon dioxide and methane fluxes from mounds of African fungus-growing termites. *Biogeosciences*, *20*(19), 4029–4042. https://doi.org/10.5194/bg-20-4029-2023

Rosenberg, Y., Bar-On, Y. M., Fromm, A., Ostikar, M., Shoshany, A., Giz, O., & Milo, R. (2023). The global biomass and number of terrestrial arthropods. *Science Advances*, *9*(5), eabq4049–eabq4049. https://doi.org/10.1126/sciadv.abq4049

Rouland, C., Brauman, A., Labat, M., & Lepage, M. (1993). Nutritional factors affecting methane emission from termites. *Chemosphere*, *26*(1–4), 617–622. https://doi.org/10.1016/0045-6535(93)90447-D

Sanderson, M. G. (1996). Biomass of termites and their emissions of methane and carbon dioxide: A global database. *Global Biogeochemical Cycles*, *10*(4), 543–557. https://doi.org/10.1029/96GB01893

Saunois, M., Stavert, A. R., Poulter, B., Bousquet, P., Canadell, J. G., Jackson, R. B., Raymond, P. A., Dlugokencky, E. J., Houweling, S., Patra, P. K., Ciais, P., Arora, V. K., Bastviken, D., Bergamaschi, P., Blake, D. R., Brailsford, G., Bruhwiler, L., Carlson, K. M., Carrol, M., … Zhuang, Q. (2020). The Global Methane Budget 2000–2017. *Earth System Science Data*, *12*(3), 1561–1623. https://doi.org/10.5194/essd-12-1561-2020

Seibold, S., Rammer, W., Hothorn, T., Seidl, R., Ulyshen, M. D., Lorz, J., Cadotte, M. W., Lindenmayer, D. B., Adhikari, Y. P., Aragón, R., Bae, S., Baldrian, P., Barimani Varandi, H., Barlow, J., Bässler, C., Beauchêne, J., Berenguer, E., Bergamin, R. S., Birkemoe, T., … Müller, J. (2021). The contribution of insects to global forest deadwood decomposition. *Nature*, *597*(7874), 77–81. https://doi.org/10.1038/s41586-021-03740-8

Seiler, W., Conrad, R., & Scharffe, D. (1984). Field studies of methane emission from termite nests into the atmosphere and measurements of methane uptake by tropical soils. *Journal of Atmospheric Chemistry*, *1*(2), 171–186. https://doi.org/10.1007/BF00053839

Singh, K., Muljadi, B. P., Raeini, A. Q., Jost, C., Vandeginste, V., Blunt, M. J., Theraulaz, G., & Degond, P. (2019). The architectural design of smart ventilation and drainage systems in termite nests. Science Advances, 5(3), eaat8520. https://doi.org/10.1126/sciadv.aat8520

Sparks, A. (2018). "nasapower: A NASA POWER Global Meteorology, Surface Solar Energy and Climatology Data Client for R." The Journal of Open Source Software, 3(30), 1035. doi:10.21105/joss.01035.

Sugimoto, A., Inoue, T., Kirtibutr, N., & Abe, T. (1998). Methane oxidation by termite mounds estimated by the carbon isotopic composition of methane. *Global Biogeochemical Cycles*, *12*(4), 595–605. https://doi.org/10.1029/98GB02266

Van Asperen, H., Alves-Oliveira, J. R., Warneke, T., Forsberg, B., Carioca De Araújo, A., & Notholt, J. (2021). The role of termite CH4 emissions on the ecosystem scale: A case study in the Amazon rainforest. *Biogeosciences*, *18*(8), 2609–2625. https://doi.org/10.5194/bg-18-2609-2021

Van Teeseling M. C. F, Pol A., Harhangi H. R., van der Zwart S., Jetten M. S. M, Op den Camp H. J. M., van Niftrik L. (2014). Expanding the Verrucomicrobial Methanotrophic World: Description

of Three Novel Species of Methylacidimicrobium gen. nov. *Appl Environ Microbiol,* 80(21). https://doi.org/10.1128/AEM.01838-14.

Vesala, R., Räsänen, M., Leitner, S., Mulat, D. G., Mwangala, L., Rikkinen, J., & Arppe, L. (2023). Mound architecture and season affect concentrations of CO_2, CH_4 and N_2O in nests of African fungus-growing termites. *Ecological Entomology*, *48*(6), 725–737. https://doi.org/10.1111/een.13267

Wijas, B.J., Lim, S. and Cornwell, W.K. (2022), Continental-scale shifts in termite diversity and nesting and feeding strategies. Ecography, 2022:. https://doi.org/10.1111/ecog.05902

Yatsko, A.R., Wijas, B., Calvert, J., Cheesman, A.W., Cook, K., Eggleton, P., Gambold, I., Jones, C., Russell-Smith, P., & Zanne, A.E. (2024). Why are trees hollow? Termites, microbes and tree internal stem damage in a tropical savanna. Functional Ecology, 39,770–782. https://doi.org/10.1111/1365-2435.14727.

Yatsko, A. R., Flores-Moreno, H., Fitzgerald, M., Zanne, A. E. (2025). Rotten to the core? Drivers of the vertical profile and accumulation of internal tree stem damage. Functional Ecology, 00, 1–15. https://doi.org/10.1111/1365-2435.70061.

Zanne, A. E., Flores-Moreno, H., Powell, J. R., Cornwell, W. K., Dalling, J. W., Austin, A. T., Classen, A. T., Eggleton, P., Okada, K., Parr, C. L., Adair, E. C., Adu-Bredu, S., Alam, M. A., Alvarez-Garzón, C., Apgaua, D., Aragón, R., Ardon, M., Arndt, S. K., Ashton, L. A., … Zalamea, P.-C. (2022). Termite sensitivity to temperature affects global wood decay rates. *Science*, *377*(6613), 1440–1444. https://doi.org/10.1126/science.abo3856

Zhou, Z., Chen, J., Cao, H., Han, P., & Gu, J. D. (2015). Analysis of methane-producing and metabolizing archaeal and bacterial communities in sediments of the northern South China Sea and coastal Mai Po Nature Reserve revealed by PCR amplification of mcrA and pmoA genes. Frontiers in microbiology, 5, 789. https://doi.org/10.3389/fmicb.2014.00789

Zhou, Y., Staver, A. C., & Davies, A. B. (2022). Species-level termite methane production rates. *Ecology*, *104*(2), e3905. https://doi.org/10.1002/ecy.3905

Zhu B., Karwautz C., Andrei S., Klingl A., Pernthaler J., Lueders T. (2022). A novel *Methylomirabilota* methanotroph potentially couples methane oxidation to iodate reduction. *mLife*, 1, 323–328. https://doi.org/10.1002/mlf2.12033

Zimmerman, P. R., Greenberg, J. P., Wandiga, S. O., & Crutzen, P. J. (1982). Termites: A Potentially Large Source of Atmospheric Methane, Carbon Dioxide, and Molecular Hydrogen. *Science*, *218*(4572), 563–565. https://doi.org/10.1126/science.218.4572.563

Supplementary Information

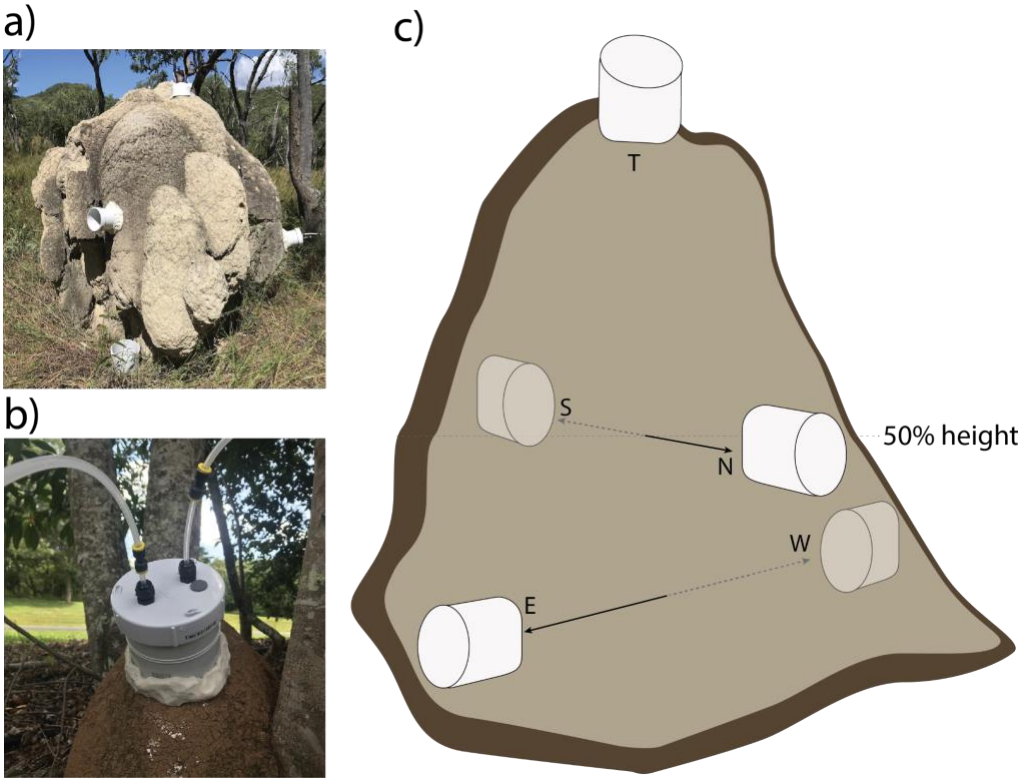

Supplementary Figure 1. Diagram of chamber-based sampling for larger mounds (five measurement points, for *C. acinaciformis* and *N. magnus*). a) A *N. magnus* mound in the field with sampling chambers fixed in place. b) The semi-closed sampling chamber system uses an external ring of potting clay to maintain airtight conditions. Tubing coming out from the chamber connects to the LGR UGGA. c) Schematic for sampling larger mounds at five locations on each mound: north-facing (N), east-facing (E), south-facing (S), west-facing (W), and top (T). Note that in the case of *A. laurensis* mounds, the top (T) measurement was omitted.

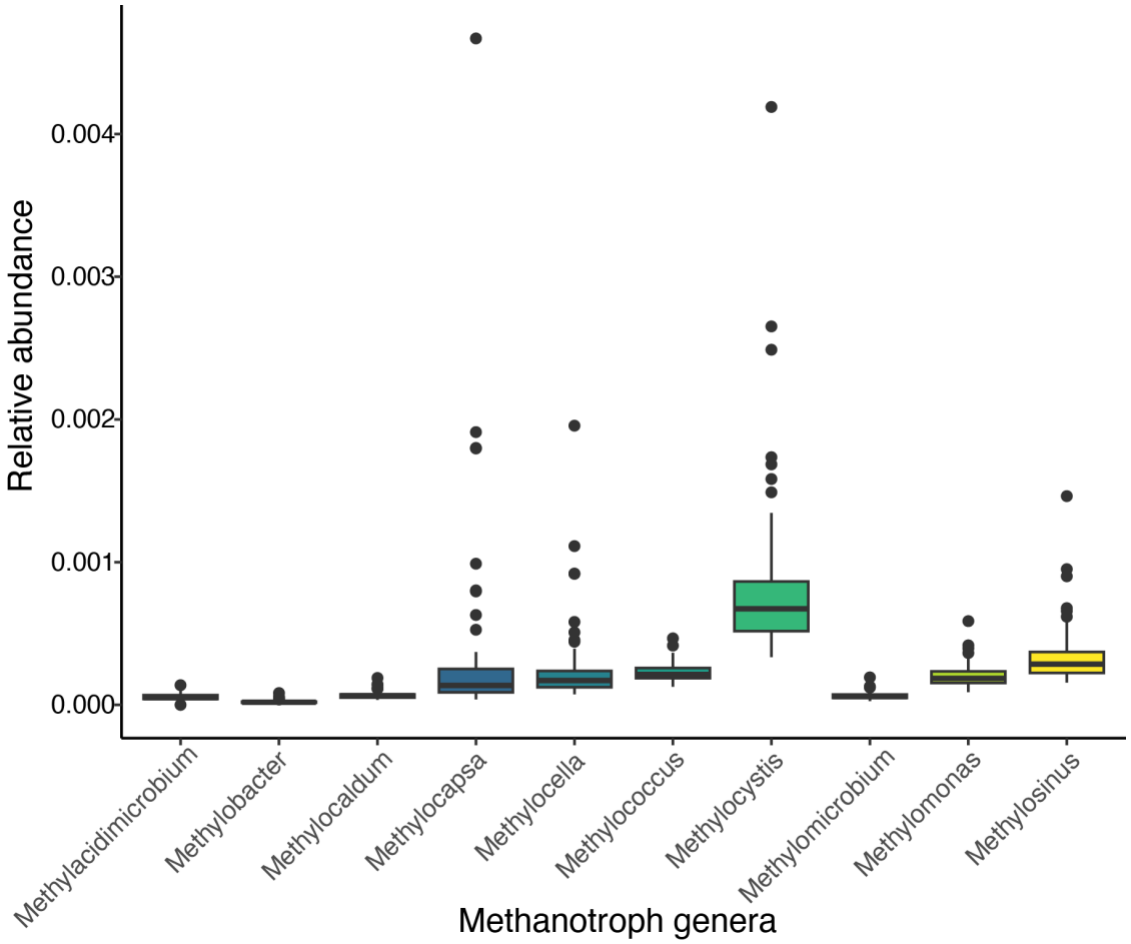

Supplementary Figure 2. Relative abundance of the ten methanotroph genera identified in the mound material metagenomic dataset for evaluating variation between mounds.

Supplementary Table 1. Environmental conditions and mound CH_4 emission sample sizes for the four resampling campaigns based on season. Monthly average temperatures for May 2022, November 2022, and August 2023 were derived from a weather station at the field site. The average temperature in February 2024 was sourced from the NASA POWER dataset using the R package 'nasapower' (Sparks 2018) due to the fact that in December 2023 Cyclone Jasper destroyed the field site weather station. Precipitation data for each season is calculated as the 1 month average precipitation prior to field sampling and was sourced from the Australian Bureau of Meteorology (BOM 2024).

Sampling campaign		Environmental conditions		Total mounds measured		
Date	Season	Temperature (C)	Precipitation (mm, 1 month average)	*A. laurensis* (n)	*C. acinaciformis* (n)	*N. magnus* (n)
May 2022	Wet-to-dry	22.4	129.9	14	25	21
Nov 2022	Dry-to-wet	26.3	28.0	8	8	8

Aug 2023	Dry	19.2	17.1	8	8	8
Feb 2024	Wet	25.1	160.2	8	8	7

Supplementary Table 2. Description of mounds remeasured across the four sampling campaigns. Bolded mound IDs indicate mounds that were successfully measured in each of the four campaigns. If a mound was destroyed or died, it is indicated when this occurred and what mound served as the replacement.

Species	Mound ID	May 2022 measurement	November 2022 measurement	August 2023 measurement	February 2024 measurement
A. laurensis	**MD10**	X	X	X	X
	MD15	X	X	X	X
	MD21	X	X	Removed, replaced by MD22	n/a
	MD24	X	X	X	X
	MD36	X	X	X	X
	MD37	X	X	X	X
	MD42	X	X	X	X
	MD54	X	X	X	X
	MD22	X	n/a	X	X
C. acinaciformis	**MD2**	X	X	X	X
	MD26	X	X	X	X
	MD27	X	X	X	X
	MD35	X	X	X	Removed, replaced by MD9
	MD48	X	X	X	X

	MD55	X	X	X	X
	MD59	X	X	X	X
	MD63	X	X	X	X
	MD9	X	n/a	n/a	X
N. magnus	**MD11**	X	X	X	X
	MD25	X	X	X	X
	MD50	X	X	X	X
	MD52	X	X	X	Removed, not replaced
	MD56	X	X	Removed, replaced by MD32	n/a
	MD57	X	X	Removed, replaced by MD61	n/a
	MD58	X	X	X	X
	MD65	X	X	X	X
	MD32	X	n/a	X	X
	MD61	X	n/a	X	X

Supplementary Table 3. Summary statistics for post hoc pairwise comparisons to determine significant species-level differences in TEF values. Bolded p-values indicate significant pairwise contrasts.

Species contrast	estimate	SE	df	t ratio	p-value
A. laurensis - C. acinaciformis	-0.343	0.104	12	-3.291	**0.02***
A. laurensis - N. magnus	0.360	0.104	12	3.450	**0.01***

C. acinaciformis - *N. magnus*	0.703	0.104	12	6.741	**0.0001***

Supplementary Table 4. Summary statistics for post hoc pairwise comparisons to determine significant differences between mound-level CH_4 emissions for the three study species. Bolded p-values indicate significant pairwise contrasts.

Species contrast	estimate	SE	df	t ratio	p-value
A. laurensis - *C. acinaciformis*	-107	534	134	-0.201	0.98
A. laurensis - *N. magnus*	0.360	549	135	-5.786	**< 0.0001***
C. acinaciformis - *N. magnus*	0.703	501	121	-6.126	**< 0.0001***

Supplementary Table 5. Results summarised across all levels of CH_4 emission: termite individual (TEF), average mound-level (per mound), and landscape scale (per hectare). Average TEF units: μg CH_4 g^{-1} termite h^{-1}. Average mound emission units: Tg CH_4 $mound^{-1}$ yr^{-1}. Landscape-scale mound emission units: Tg CH_4 ha^{-1} yr^{-1}. Asterisks (*) in the average TEF, average mound-level emission, and landscape-scale mound emission columns indicate the top-emitting species at each level of inference (individual, mound, landscape).

Species	Feeding group	Average TEF	Mounds occupied ha^{-1}	Average mound-level emission	SD mound-level emission	Landscape-scale mound emissions
A. laurensis	plant leaf litter	0.73	120.4	8.64×10^{-12}	1.01×10^{-11}	1.04×10^{-9}*
C. acinaciformis	wood	1.07*	2.8	6.04×10^{-11}	4.64×10^{-11}	1.69×10^{-10}
N. magnus	grass	0.37	5.6	1.46×10^{-10}*	1.03×10^{-10}	8.17×10^{-10}
All species	**–**	**0.72**	**128.8**	**7.16×10^{-11}**	**5.32×10^{-11}**	**2.03×10^{-9}**

Supplementary Table 6. Summary of structural equation modeling (SEM) output.

Response	Predictor	Estimate	Std. Error	DF	t-value	P-value
Mound volume	species_s	–	–	2	0.00	1.00
	species_s = N. magnus	0.00	0.22	73	0.00	1.00
	species_s = C. acinaciformis	0.00	0.19	73	0.00	1.00

	species_s = A. laurensis	0.00	0.19	73	0.00	1.00
Mound wall thickness	species_s	–	–	2	0.00	1.00
	species_s = A. laurensis	0.00	0.19	73	0.00	1.00
	species_s = C. acinaciformis	0.00	0.19	73	0.00	1.00
	species_s = N. magnus	0.00	0.22	73	0.00	1.00
Mean mound CH_4 emission	volume_m3_st	-169.47	458.58	14.34	-0.37	0.71
	wt_mm_st	278.80	455.62	14.00	0.61	0.55
	temp	112.76	52.58	59.23	2.14	**0.04***
	species_s	–	–	2	3.36	0.06
	species_s = A. laurensis	2218.80	720.44	13.97	3.08	**0.008***
	species_s = C. acinaciformis	2747.25	719.77	13.93	3.82	**0.002***
	species_s = N. magnus	5026.98	856.97	14.25	5.87	**<0.0001***
	campaign	–	–	3	4.52	**0.007***
	campaign = nov22	2474.04	645.34	45.16	3.83	**0.0004***
	campaign = feb24	2709.90	557.92	31.98	4.86	**<0.0001***
	campaign = aug23	3696.92	684.67	50.19	5.40	**<0.0001***
	campaign = may22	4443.18	542.64	29.56	8.19	**<0.0001***

Supplementary Table 7. Model summary of linear mixed effects model testing all relevant predictors of CH_4 emission to understand variation across mounds. For termite species-level comparisons, *A. laurensis* is the reference species.

Fixed effects	Estimate	Std. Error	df	t value	p
intercept	3054.89	1539.61	34.74	1.98	0.06
pmoA relative abundance	-274.52	422.67	39.53	-0.65	0.52
Species - *C. acinaciformis*	-821.89	1775.22	18.48	-0.46	0.65
Species - *N. magnus*	1222.07	1764.64	18.10	0.70	0.50
PCoA1	16524.09	15631.67	38.13	1.06	0.30

PCoA2	2939.86	221396.66	45.78	0.14	0.89
Relative abundance methanotroph sum	284927.70	384117.34	38.62	0.74	0.46
PCoA1 * PCoA2	-392290.96	526711.81	39.67	-0.75	0.46

Supplementary Table 8. Model results for testing individual methanotroph genera relative abundance as a predictor of CH_4 emission. Bolded values indicate significance.

Methanotroph genera	Fixed effect	Estimate	SE	df	t	p
Methylacidimicrobium	Intercept	3816	1426	28.94	2.676	**0.01***
	Methanotroph genera	266100	13030000	40.21	0.02	0.98
	speciesC.acinaciformis	-839.1	1753	17.53	-0.479	0.64
	speciesN.magnus	1130	1770	18.11	0.638	0.5
Methylobacter	Intercept	4026	1325	22.81	3.039	**0.006***
	Methanotroph genera	-1E+07	25250000	41.84	-0.402	0.69
	speciesC.acinaciformis	-756.8	1754	17.92	-0.431	0.67
	speciesN.magnus	1131	1760	18.07	0.643	0.53
Methylocaldum	Intercept	3838	1419	28.37	2.704	**0.01***
	Methanotroph genera	-108200	10680000	40.83	-0.01	0.99
	speciesC.acinaciformis	-836.9	1757	17.64	-0.476	0.64
	speciesN.magnus	1130	1770	18.07	0.638	0.53
Methylocapsa	Intercept	3794.45	1247.62	17.74	3.041	**0.007***
	Methanotroph genera	165119.4	439592.2	41.34	0.376	0.71
	speciesC.acinaciformis	-892.29	1765.06	17.77	-0.506	0.62

	speciesN.magnus	1122.7	1776.35	18.14	0.632	0.534
Methylocella	Intercept	3785.87	1259.42	18.5	3.006	**0.007***
	Methanotroph genera	213799.9	999328.4	41.29	0.214	0.83
	speciesC.acinaciformis	-863.23	1760.32	17.69	-0.49	0.63
	speciesN.magnus	1123.38	1773.83	18.15	0.633	0.53
Methylococcus	Intercept	4042.57	1556.12	37.61	2.598	**0.01***
	Methanotroph genera	-953640	4254134	39.83	-0.224	0.82
	speciesC.acinaciformis	-819.63	1749.6	17.6	-0.468	0.65
	speciesN.magnus	1128.31	1764.95	18.12	0.639	0.53
Methylocystis	Intercept	3830.74	1290.73	20.42	2.968	**0.007***
	Methanotroph genera	-216.34	475866.5	41.55	0	1.00
	speciesC.acinaciformis	-838.06	1757.3	17.7	-0.477	0.64
	speciesN.magnus	1129.87	1770.51	18.15	0.638	0.53
Methylomicrobium	Intercept	3928	1393	27.03	2.819	**0.009***
	Methanotroph genera	-1641000	10820000	40.24	-0.152	0.88
	speciesC.acinaciformis	-817	1756	17.77	-0.465	0.65
	speciesN.magnus	1129	1767	18.15	0.639	0.53
Methylomonas	Intercept	3984.84	1408.84	28.05	2.828	**0.009***
	Methanotroph genera	-781010	3419619	40.48	-0.228	0.82

	speciesC.acinaciformis	-819.41	1750.41	17.61	-0.468	0.65
	speciesN.magnus	1126.76	1765.81	18.14	0.638	0.53
Methylosinus	Intercept	3834.32	1315.65	21.88	2.914	**0.008***
	Methanotroph genera	-11625.3	1367944	41.72	-0.008	0.99
	speciesC.acinaciformis	-837.26	1756.09	17.66	-0.477	0.64
	speciesN.magnus	1129.93	1770.4	18.15	0.638	0.53

Supplementary Table 9. Model summary of linear mixed effects model testing all relevant predictors of CH_4 emission to understand variation within mounds. For termite species-level comparisons, *A. laurensis* is the reference species.

Fixed effects	Estimate	Std. Error	df	t value	p
intercept	5470.08	1904.12	40.64	2.87	**0.006***
pmoA relative abundance	-1225.34	678.22	32.63	-1.81	0.08
Species - *C. acinaciformis*	244.10	1618.62	13.41	0.15	0.88
Species - *N. magnus*	3420.91	1533.97	11.32	2.23	**0.047***
PCoA1	-13070.41	35193.02	52.13	-0.371	0.71
PCoA2	12518.02	30237.22	52.51	0.41	0.68
Relative abundance methanotroph sum	-392888.56	771264.09	53.64	-0.51	0.61
PCoA1 * PCoA2	469113.2	601090.41	53.34	-0.78	0.43

Supplementary Table 10. Summary of published CH_4 emissions for termite mounds at the species level. Note that the sample sizes from this study include mounds that were a part of the initial, larger sampling campaign, hence the greater sample size for each species.

Study	Species	n	Mound-level emission (μmol CH_4 h^{-1} $mound^{-1}$)	Average total mound volume (m^3)
This study (Australia)	*Amitermes laurensis*	14	57.11 (average)	0.04
	Coptotermes acinaciformis	25	304.79 (average)	0.80
	Nasutitermes magnus	19	1290.23 (average)	0.94
Van Asperen et al. 2021 (Brazilian Amazon)	*Neocapritermes brasiliensis*	5	61-125 (range)	0.05
Khalil et al., 1990 (Australia)	*Amitermes laurensis*	n/a	67.39 (average)	n/a
	Drepanotermes perniger	3-5	134.78 (average)	n/a
	Nasutitermes magnus	3-5	112.32 (average)	n/a
	Nasutitermes triodae	3-5	89.86 (average)	n/a
	Tumulitermes pastinator	3-5	67.39 (average)	n/a
	Coptotermes lacteus	2	8.99 (average)	n/a
Macdonald et al., 1998 (Cameroon)	*Bulbitermes sp. C*	3	8.83 (average)	n/a
	Dicuspiditermes nemorosus	6	10.91 (average)	n/a
	Dicuspiditermes santschii	12	20.69 (average)	n/a
	Prohamitermes mirabilis	2	0.32 (average)	n/a
Martius et al., 1993 (Brazilian Amazon)	*Nasutitermes ephratae*	5	172.07 (average)	0.03
	Nasutitermes macrocephahts	1	24.94	0.007
	Nasutiteones surinamensis	2	177.68 (average)	0.03
	Nasutitermes comiger	1	12.47	0.001

	Nasutitermes araujoi	1	143.39	0.04
Seiler et al., 1984 (South Africa)	*Odontotermes sp.*	3	4.36 (average)	n/a
	Macrotermes sp.	5	168.33 (average)	n/a
	Cubitermes sp.	7	1.43 (average)	n/a
	Amitermes sp.	17	4.99 (average)	n/a
	Hodotermes sp.	3	4.30 (average)	n/a
	Trinervitermes sp.	10	642.14 (average)	n/a
Sugimoto et al., 1998 (Thailand)	*Microcerotermes sp.*	2	1.59 (average)	n/a
	Globitermes sulphures	1	1.79	n/a
	Termes sp.	1	0.71	n/a
	Dicuspiditermes sp	3	0.65 (average)	n/a

Supplementary Table 11. List of bacterial genera associated with methanotrophy. These genera were used to query the metagenomics dataset for methanotroph candidates to include in our analysis on variation in bacterial methanotroph community composition within and between mounds.

Genera	**Reference**
Methylobacter	Zhou et al., 2015
Methylomonas	Bowman et al., 1993
Methylosarcina	Kalyuzhnaya 2016a
Methylomicrobium	Kalyuzhnaya 2016b
Methylococcus	Bowman et al., 1993
Methylocystis	Bowman et al., 1993

Methylosinus	Bowman et al., 1993
Methylacidiphilum	Awala et al., 2023
Methylacidimicrobium	van Teeseling et al., 2014
Methylomirabilis	Zhu et al., 2022
Methylocapsa	Dunfield et al., 2010
Methylocella	Dunfield et al., 2010
Methylohalobius	Dunfield 2016
Methylothermus	Houghton et al., 2019
Methylosphaera	Bowman 2015
Methylocaldum	Delherbe et al., 2024

1005